Methods for the High Resolution Analysis of Glycoconjugates

Christopher Gray and Sabine L. Flitsch

Abstract Glycans and their conjugates form the largest and most diverse class of biological molecules found in nature. These glycosides are vital for numerous cellular functions including recognition events, protein stabilisation and energy storage. Additionally, abnormalities within these structures are associated with a wide range of disease states. As a result, robust analytical techniques capable of in depth characterisation of carbohydrates and their binding partners are required. This chapter provides an overview of currently used analytical techniques, focussing on chromatographic and mass spectrometry-based methods.

1 Introduction

Glycosylation involves the enzymatic transfer of a carbohydrate from a donor molecule to a substrate such as a protein, lipid or another carbohydrate, forming elongated and often branched glycoconjugate structures. Diverse varieties of these glycoconjugates coat the surface of all cells and act as receptors for glycan-binding species such as lectins, antibodies or pathogens [1, 2]. Glycosylation is the most prevalent post-translational modification (PTM) observed within nature; in fact, it is thought that greater than half of all known proteins are glycosylated [3]. It is widely reported that these glycans are vital for regulation of many biological interactions such as cell–cell recognition, [4] cell adhesion [5], immune response [6], infection [7, 8] and fertilisation [9–11]. It has also been shown that aberrant glycosylation is related to several diseases including cancer [12–17], muscular dystrophy [5] and pancreatitis [18, 19]. Even subtle changes in carbohydrate structure can result in vastly different interactions, make them susceptible to proteolysis or alter glycoconjugate tertiary structures and thus affects the observed biological response [5, 15, 17, 20–25]. It remains unclear a priori how changes within a glycan structure

C. Gray · S.L. Flitsch (✉)
School of Chemistry and Manchester Institute of Biotechnology, The University of Manchester, 131 Princess Street, Manchester M1 7DN, UK
e-mail: sabine.flitsch@manchester.ac.uk

Z.J. Witczak and R. Bielski (eds.), *Coupling and Decoupling of Diverse Molecular Units in Glycosciences*, https://doi.org/10.1007/978-3-319-65587-1_11

will affect the resultant biological function [26]. Knowledge of these structure–function relationships could enable the development of novel therapeutics or diagnostics [27–29]. Additionally, carbohydrates are foreseen as routes to novel fuels and materials [30–32], providing further requirement for rigorous analytical approaches to characterise them.

However, there are inherent difficulties in analysing the 'glycome', the entire complement of glycans and their glycoconjugates produced by an organism under specified conditions of time, space and environment [2], compared to the widely researched genome and proteome. Firstly, glycan structures are not directly encoded from genetic information. Moreover, glycosylated macromolecules tend to exist in multiple glycoforms and are often low abundant compared to their non-glycosylated counterparts, thus requiring enrichment prior to analysis. These glycoforms vary depending on conditions, such as disease state [18], age [33], and gender [9, 34] further increasing the complexity of glycome analysis. Finally, the elucidation of glycan chemical structures using most analytical techniques is extremely challenging. Glycans can be composed of a far greater number of natural monosaccharide building blocks (several hundred) compared to the 4 nucleotides and 20 essential amino acids found in DNA and proteins, respectively [2], although there is a core of 10 major monosaccharide units found within vertebrates (Fig. 1).

These monosaccharide building blocks are often stereo- or regio-isomers of one another (unlike nucleotides or amino acids) making their characterisation more

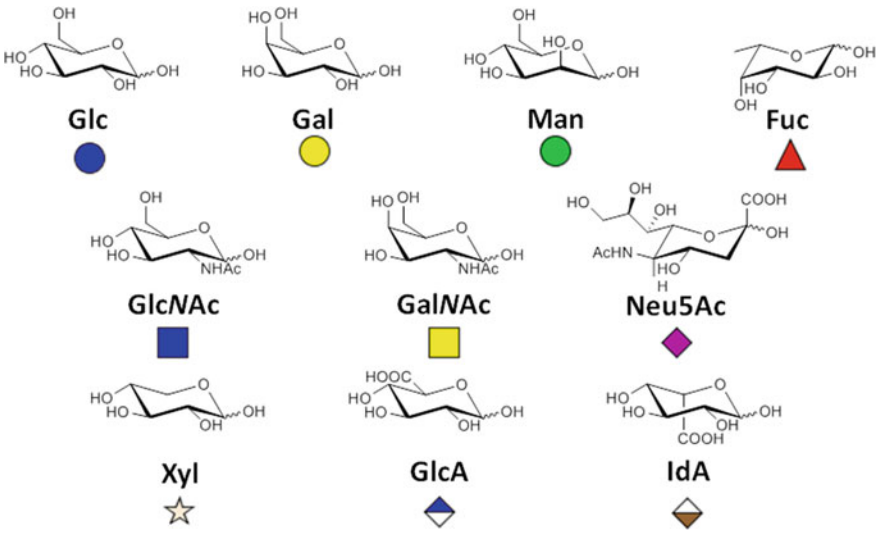

Fig. 1 The common monosaccharides found in vertebrates including the shorthand used by the Consortium for Functional Glycomics. Glc = Glucose, Gal = Galactose, Man = Mannose, Fuc = Fucose, Glc*N*Ac = *N*-Acetylglucosamine, Gal*N*Ac = *N*-Acetylgalactosamine, Xyl = Xylose, GlcA = Glucuronic acid, IdA = Iduronic acid and Neu5Ac = *N*-acetylneuraminic acid. Glc, Gal and Man isomers form the hexoses (Hex), Glc*N*Ac and Gal*N*Ac isomers the *N*-acetylhexosamines and GlcA and IdA isomers the hexuronic acids

analytically challenging [35]. Additionally, the glycosidic bond formed between monosaccharides can adopt two different configurations, namely α- and β-, where the binding monosaccharide lies either above the plane of ring, or planar to the ring, respectively (Fig. 2). This linkage can also form at several positions resulting in the formation of branched structures, which are primarily linear combinations of amino acids and nucleotides, respectively [2, 36, 37]. Finally, these carbohydrate rings can potentially exist as furanose or pyranose forms.

There are two common types of protein glycosylation, (not to be confused with the chemically similar process glycation which occurs non-enzymatically): *N*-glycosylation and *O*-glycosylation. Typical eukaryotic *N*-glycosylation involves enzymatic *en bloc* transfer of the glycan $Glc_3Man_9GlcNAc_2$ from dolichol phosphate to asparagine residues within in the consensus peptide sequence Asn-Xxx-Ser/Thr (where Xxx is any amino acid except proline) [2, 38, 39]

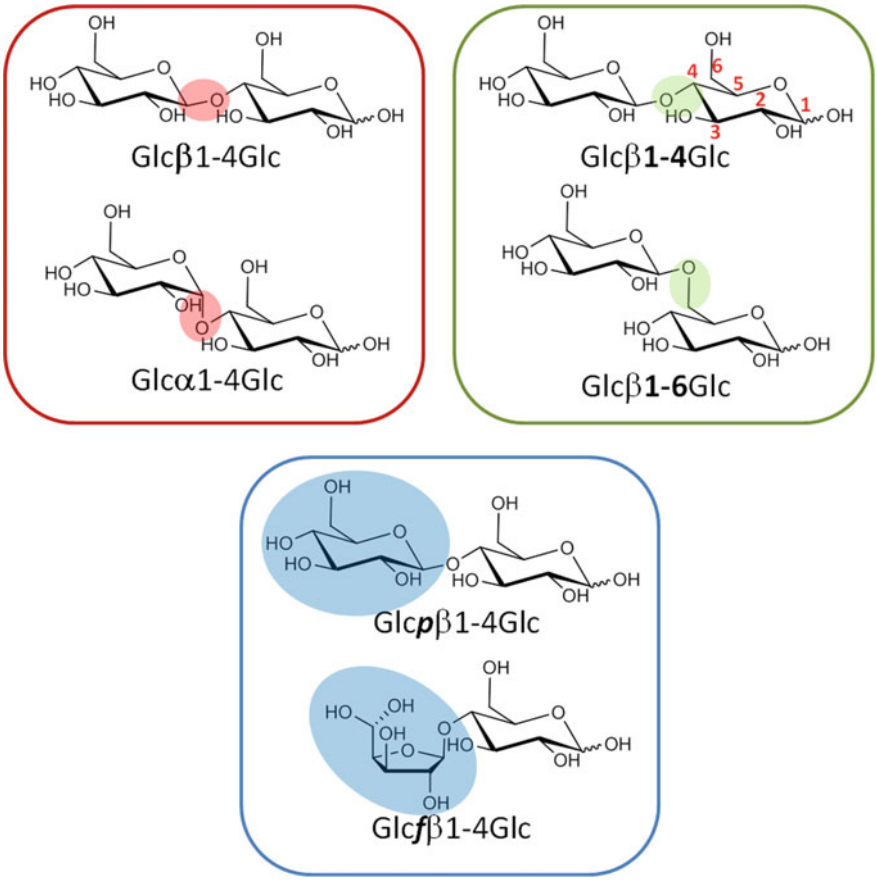

Fig. 2 Scheme depicting two α-/β-stereoisomers (*red*), two regioisomers (*green*) and two pyranose/furanose isomers (*blue*)

although this is not always the case [3]. The $Glc_3Man_9GlcNAc_2$ modification is synthesised first on the cytoplasmic face of the endoplasmic reticulum (ER) membrane in a stepwise manner from dolichol phosphate to $Man_5GlcNAc_2$, This is then 'flipped' so that it faces into the ER lumen, where additional glycosyl transferases modify this species producing $Glc_3Man_9GlcNAc_2$ that is then transferred in a co-translational event *en bloc*, mediated by an oligosaccharyltransferase, to the asparagine acceptor of the forming polypeptide chain [2, 40]. Various glycosidases and glycosyltransferases further modify this glycoconjugate within the Golgi apparatus, generating a structure that can be classed as one of three classes (Fig. 3): **high mannose**, where the *N*-glycan core ($Man_3GlcNAc_2$) is comprised of only branched Man and Glc*N*Ac residues; **complex** where the cores antennae are functionalised with other saccharides including galactose, fucose and sialic acid; and **hybrid** where a single antennae from the core structure is functionalised with mannose residues (α1–6 arm) and the others with complex structures. *N*-glycosylation primarily occurs on secreted or membrane-bound proteins within eukaryotes or archaea [41] and was later shown to occur on proteins within the Gram-negative bacterium *Campylobacter jejuni* [42]. Unlike *N*-glycosylation in eukaryotes, there is no conserved carbohydrate sequence transferred *en bloc* to proteins (i.e. $Glc_3Man_9GlcNAc_2$ for eukaryotes), although certain motifs seem to be important such as the presence of a reducing acetamido group for bacterial *N*-oligosaccharide transferases [40]. Also archaea and bacterial *N*-glycans are structurally different compared to eukaryotic *N*-glycans possessing, for example, hexuronic acids or bacilosamine residues, respectively [40].

O-glycosylation occurs post-translationally onto the –OH group of typically serine or threonine residues within proteins. Unlike *N*-glycans, *O*-glycans are synthesised stepwise on glycoproteins and tend to be much shorter than their *N*-glycan counterparts consisting of just a single residue in some cases [38]. Within Eukaryotes, initial transfer of α-Gal*N*Ac, which is the most common addition, and α-Fuc to proteins occurs in the Golgi, whereas *O*-mannosylation is initiated in the ER and *O*-Glc*N*Acylation and glucosylation occurs in the cytosol (and nucleus for *O*-Glc*N*Ac) [2, 38, 43]. These carbohydrates may then be extended by a series of glycosyltransferases in the Golgi. For the most common type of *O*-glycosylation, *O*-Gal*N*Ac, a series of eight common core structures exist (Fig. 4). Unlike *N*-glycosylation no consensus motif has yet been identified for *O*-glycosylation, making *O*-glycosylation site identification more challenging [44]. For specific classes of *O*-glycosylation though, protein sequence preferences have been identified allowing prediction of potential *O*-glycosylation sites [45]. Certain proteins, known as mucins, are heavily *O*-glycosylated with Gal*N*Ac: these will be the focus of Chap. "[3,3]-Sigmatropic Rearrangement as a Powerful Synthetic Tool on Skeletal Modification of Unsaturated Sugars".

Glycan structures are routinely assigned using minimal analytical information, based on the assumption that their biosynthetic pathways are highly conserved, which is not necessarily always the case [19, 46, 47]. Alternatively, structures can be directly elucidated to varying degrees by NMR, tandem mass spectrometry or sequential glycosidase treatment followed by chromatographic separation [15, 46, 48–50]. However, these approaches are limited by either sensitivity or specificity.

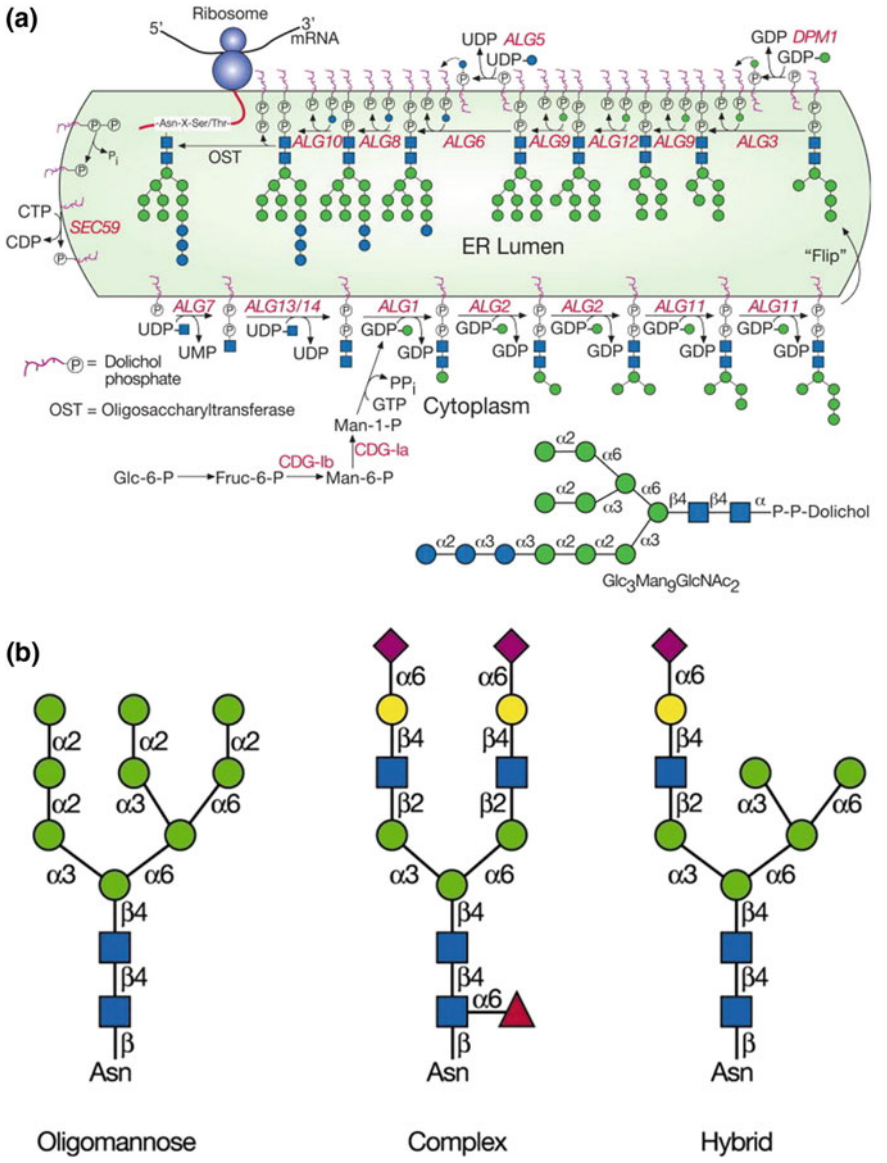

Fig. 3 The biosynthetic pathway by which the oligomannose structure transferred to proteins forming *N*-glycans is generated (**a**). Various glycosidases and glycosyltransferases then act on this glycan to produce the different types of *N*-glycans observed within eukaryotic organisms (**b**). Figures are taken from Varki et al. [2]

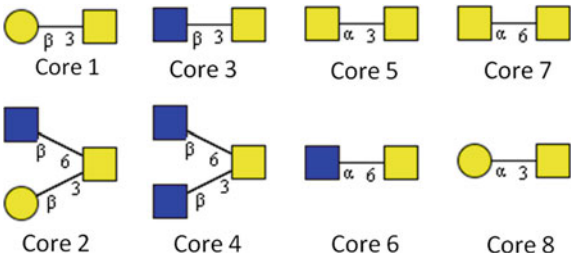

Fig. 4 Basic core *O*-Gal*N*Acylated structures [44]

Consequently, high-throughput analytical methodologies capable of sequencing glycan structures and further identifying protein binding partners are highly sought after. Mass spectrometry (MS)-based techniques offer the capability of elucidating structural information on a wide range of biological analytes including peptides, proteins and glycans in a high-throughput manner. However, they are often unable to unambiguously assign carbohydrate structures given that most monomeric building blocks are simple epimers of one another. Integration of ion mobility spectrometry, a technique that separates ions by their rotationally averaged collision cross section, with (tandem) mass spectrometry offers the potential capability to separate these isomeric precursors and product ions, which would greatly aid glycan characterisation. Of particular interest is the ability to separate and determine the cross section of isomeric mono-/disaccharide product ions, which crucially could be indicative of the stereochemistry of the residue, the anomeric configuration, ring size and regiochemistry. Therefore, IM-MS has the potential to fill a gap in the Glycomics community, namely a high-throughput carbohydrate sequencing strategy.

High-throughput strategies to identify proteins that bind to glycans are also of great interest. Most high-throughput strategies involve arraying thousands of glycans to a solid support, incubating them with purified proteins, washing and then visualisation by fluorescence or radiation. However, these approaches rely on purified material and incorporation of a fluorescent or radioactive tag. (Tandem) Mass spectrometry of proteins adhered to the arrays, or peptides resulting from on-chip proteolysis, offers a rapid and direct means to unambiguously characterise unlabelled bound proteins, even from endogenous mixtures.

Multiple MS-based strategies underpin the ability to characterise glycans and their binding partners. Glycans and their conjugates are initially ionised, principally by matrix-assisted laser desorption ionisation (MALDI) or electrospray ionisation (ESI), as either cation or anion adducts and then can be made dissociate if required [51]. These precursor or product ions are then separated based on their mass-to-charge (*m/z*) ratio mass and subsequently detected.

2 Mass Spectrometry Techniques Applied to Glycoconjugate Analysis

2.1 Ionisation Techniques

2.1.1 Electrospray Ionisation (ESI)

Electrospray ionisation (ESI), or nanospray ESI (nESI) for nanoflow, is a soft ionisation technique, i.e. it causes little to no fragmentation of the molecules during ionisation, including large molecules such as proteins [52] and protein assemblies [53, 54]. It is also the most commonly used ionisation strategy in biomolecule analysis as it can be operated at atmospheric pressure and can be easy coupled to liquid chromatography meaning that a mixture of analytes can be separated on-line prior to ESI-MS analysis. However, samples can be directly infused by syringe pumps or static nESI tips. ESI and nESI operate at μL min^{-1} and nL min^{-1} flow rates, respectively, permitting analysis of low amounts of analyte suitable for biological samples. (n)ESI emitters are subjected to a high potential electric field (1–5 kV) [55]. At the capillary tip a large electric field is formed ($\sim 10^6$ V m^{-1}) resulting in the charged analyte solution being polarised, i.e. in positive ion mode a negative potential is applied across the capillary therefore positively charged molecules are drawn to the end of the tip. This field also causes the meniscus at the capillary nozzle to be perturbed forming a cone (Taylor cone) as shown in stage 1 Fig. 5.

When the force the electric field exerts is high enough, the tip of the Taylor cone is destabilised resulting in the formation of a jet of charged droplets that repel one another, causing them to spread out orthogonally and accelerate towards the counter electrode by electrostatic attraction [52, 57, 58]. These droplets evaporate, which may be aided by an inert drying gas such as nitrogen and elevated temperatures, until the point where the Coulombic repulsive forces of the charged analyte destabilise the droplet. This occurs slightly below the Rayleigh limit where repulsion equals the surface tension. At this point, the droplets 'explode' forming even smaller droplets. The precise mechanisms of ion formation from these droplets are not clear and are thought to be dependent on the nature of the analyte ion. Three postulated mechanisms are the ion evaporation model (IEM) [59], the charged residue model (CRM) [60] and the chain ejection model (CEM) [56, 61]. The IEM, believed to be prevalent for small molecules (e.g. glycans), involves ejection of a small analyte ion from the surface of a small (nm radius) charged droplet when the Rayleigh limit is sufficiently high. This process is kinetically disfavored for large molecule ions, which are thought to form by the CRM [56]. In the CRM, solvent continually evaporates from the droplet containing the analyte. As the final solvent shell evaporates, the remaining charge within the droplet is transferred to the analyte. During this process, analytes are charge reduced so they maintain the Rayleigh limit by IEM ejection of solvated protons and small ions [56]. Finally the CEM, which suggests unfolded 'chains' migrate to the droplet surface when the

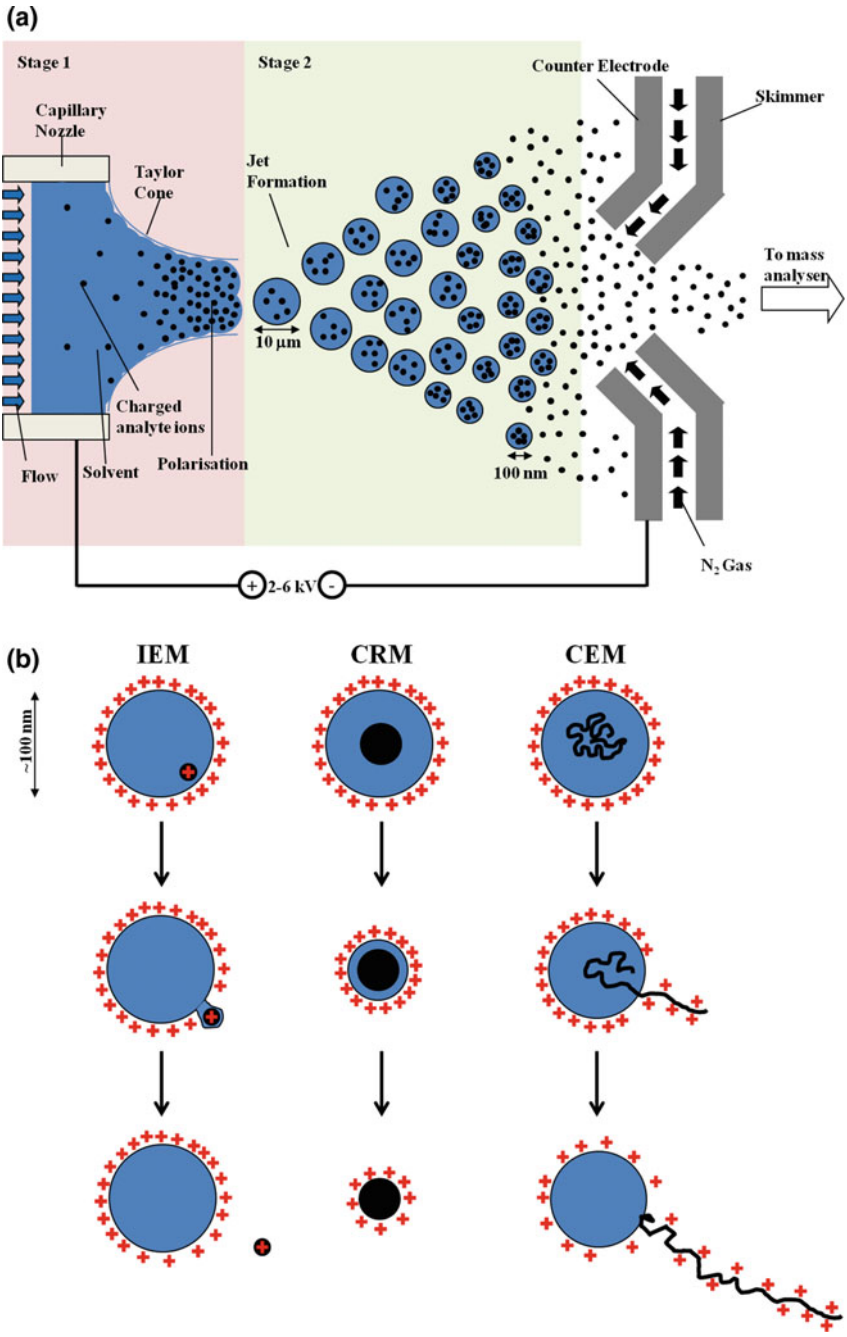

Fig. 5 Schematic depicting the ESI ionisation mechanism (**a**) and schemes depicting ion formation models for the ion evaporation model (IEM), charged residue model (CRM) and the chain ejection model (CEM) (**b**) (redrafted version of figure from Ref. [56])

Rayleigh limit is reached. This charged chain is then liable to be ejected from the surface of the droplet. Sequentially, more and more of the charged chain is ejected from the droplet until the remainder of the droplet evaporates or the entire analyte is ejected [62]. This mechanism is believed to occur for large disordered analytes, such as polymers or disordered proteins and accounts for the observed higher analyte charge states than the CRM would predict [56]. Regardless of the ion formation mechanism, the composition of the sprayed solution will impact the formed ions and as a result can perturb the measured mass spectrum. ESI solutions often contain organic solvents such as methanol or acetonitrile to lower the surface tension of electrospray droplets improving desolvation and thus ionisation. Furthermore, these solutions tend to contain volatile acids, such as formic acid, for positive ion mode or bases, such as ammonia, for negative ion mode providing a source of protons or a proton sink, respectively. Conversely, molecules can be promoted to form metal adducts by doping the solution with salts such as sodium formate or lithium chloride. Structured proteins can also be stabilised through buffering with volatile salts such as ammonium acetate [53].

ESI is advantageous as it can produce large (kDa to MDa) ions, even from non-volatile, thermally labile compounds and is typically compatible with conventional liquid chromatography techniques [52]. Also given that these ionised species are typically multiply charged, their *m/z* values tend to fall within the operating range of most mass spectrometers [58]. However, ESI, like most ionisation techniques, suffers from a low tolerance towards salts, therefore, samples must be desalted prior to analysis. Finally, as the technique is very sensitive, the spray chamber must be kept very clean to avoid contamination and signal suppression [63].

2.1.2 MALDI

Matrix-assisted laser desorption ionisation (MALDI) is, like ESI, a soft ionisation technique, although involves desorption of analyte ions from the solid phase induced by irradiation with a pulsed UV laser at 337 or 355 nm for 1–10 ns [58, 64, 65]. Interestingly, unlike ESI, analyte ions generated tend to only be singly charged, greatly simplifying mass spectra. Analytes are co-crystallised with an excess of a UV absorbing organic acid matrix (1:5000), on an inert metal (typically a stainless steel or gold) target, forming ideally homogenous crystals. The matrix has two main purposes, firstly it separates analyte molecules preventing analyte–analyte interactions that may hinder desorption and ionisation, and secondly and more importantly, it absorbs most of the UV radiation from the laser pulse protecting the analyte (Fig. 6). The matrix may also act as proton sources or sinks depending on the operation mode [66]. Different matrices work better for ionisation of different classes of analytes, so the choice of the matrix depends on the analyte being studied. For example sinapinic acid (SA) works well with proteins, α-cyano-4-hydroxycinnamic acid (CHCA) is good for small proteins and peptides, 2,4,6-trihydroxyacetophenone (THAP) is good for glycans and 2,5-dihydroxybenzoic acid (DHB) is commonly

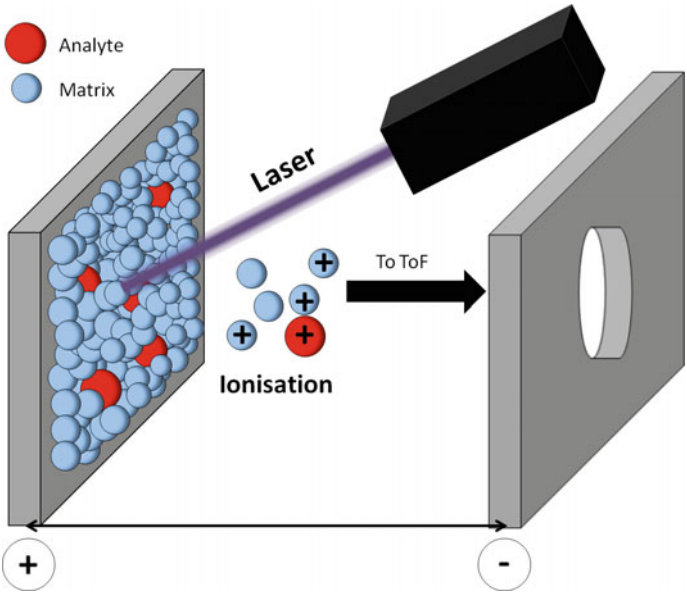

Fig. 6 Schematic of MALDI ionisation of positively charged analytes (*red*) co-crystallised with an excess of UV-absorbing matrix (*blue*)

used for all organic molecules and is particularly useful for those analytes which are labile for example, covalently modified peptides. Upon UV absorption the matrix sublimes *in vacuo* causing rapid expansion, which results in analyte and photoionised matrix molecules being ejected into the gas phase, although most remain uncharged (primary ionisation) [58, 67]. There are several models for ionisation with none being completely accepted. The two most accepted are the cluster '(refined) Lucky Survivors' and the gas-phase proton transfer [64, 68–72]. The 'Lucky Survivors' model states that the singly and multiply charged analyte ions are preformed in the matrix solution and retain their solution charge during co-crystallisation. Following a UV laser pulse, the matrix and analyte sublime and the multiply charged analyte ions undergo secondary neutralisation reactions with free electrons until they become singly charged [73]. The gas-phase protonation model suggests secondary collisions, within the MALDI plume, between the neutral analyte and charged UV matrix molecules in the gas plume results in ionisation of the analyte (secondary ionisation). The matrix charge is either preformed in solution or resulting from the laser energy being absorbed by the matrix (pooling—Coupled Chemical and Physical Dynamics model) [70, 74]. Recently, it has been reported that it is highly likely that both ionisation mechanisms are involved [73]. This ionisation technique is advantageous as it is quick and produces little fragmentation of analyte ions. However, ions produced by MALDI are metastable, and therefore are liable to dissociating during traversing the field-free region of the Time-of-Flight (ToF) mass analyser that is typically coupled with a MALDI source. Metastable

decay is more prominent for larger species whose time-of-flight is greater. This causes a loss in sensitivity due to a reduction in the number of intact analyte ions reaching the detector [55]. Nevertheless, this post-source decay can be exploited in MS^2 studies. Another disadvantage of MALDI is the limitation of analysing ions below *m/z* of 500 due to the excess number of matrix-derived ions that can saturate the signal. Salts and other buffers also hinder MALDI, although to a lesser extent compared to ESI [58, 63].

2.2 Mass Analysers

2.2.1 Quadrupole

Quadrupoles are composed of four parallel rods, ideally with a hyperbolic cross section, arranged in a diamond shape. Each opposing rod is electrically connected to one another and has the opposite polarity to the pair of rods perpendicular to them (Fig. 7). Both pairs possess a direct current (DC) potential and are overlaid with an alternating radio-frequency (RF) potential. In the case where the analyte ions are positive, when the RF and DC potential in the *x*–*z* plane is positive the analyte ions are focussed into the centre of the quadrupole.

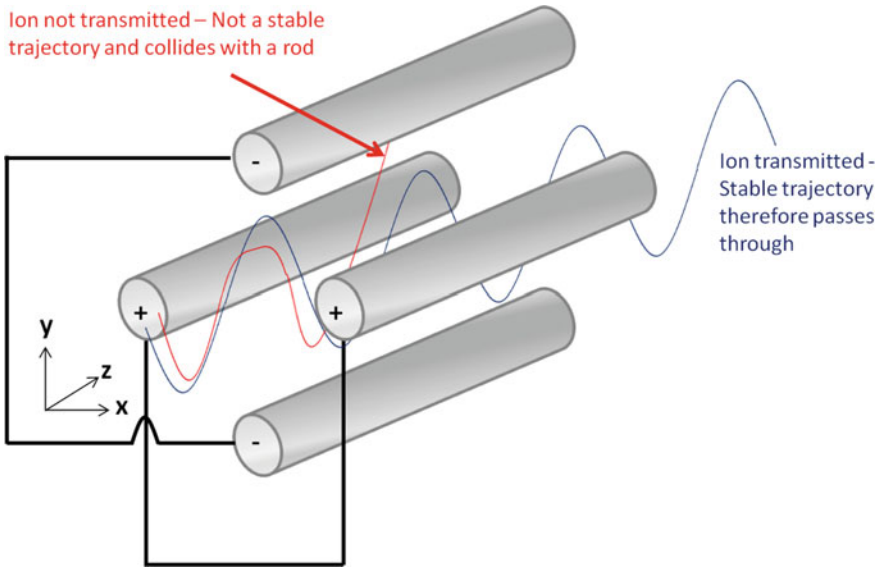

Fig. 7 Scheme depicting transmission though a quadrupole mass analyser and the respective potentials applied to the rods at a certain point in time. Depending on the magnitude and polarity of the applied potentials, certain ions of a given *m/z* posses stable trajectories and are transmitted through the quadrupole (*blue*) unlike others that collide with the rods and annihilate (*red*)

When the RF polarity switches to negative (more than the DC positivity), the ions are accelerated towards the *x*–*z* plane rods. Ions of low mass and higher charge will be accelerated more than heavier ions of lower charge and may collide with the electrodes at which point they will be discharged and pumped off as neutral species. As a result, only ions with high *m/z* are transferred (referred to as the high pass mass filter). The *y*–*z* plane rods operate at an opposite DC potential to those in the *x*–*z* plane (for this example negative). In this case, ions of large *m/z* are more likely to collide with the rods as they are less likely to respond to the focussing that occurs when the alternating RF potential becomes positive unlike ions with lower *m/z*. Therefore, only ions with a low *m/z* are transferred (the low pass mass filter). The net effect of these two filters is that only a narrow range of ions will have a stable trajectory and thus pass through the quadrupole [75]. If the DC and RF voltage is increased whilst keeping the DC to RF ratio constant, new stable trajectories will be created for ions with an increasing *m/z* value, allowing a range of ions of different *m/z* values to be scanned [58]. Controlling the DC and RF ratio plays a significant role in the resolution of this mass analyser with a lower DC to RF ratio producing a lower mass resolution. The stability of ions passing through a (hyperbolic) quadrupole field possessing both DC and RF potential can also be expressed in terms of the Mathieu equations (Eqs. 1 and 2) [75].

$$a_x = -a_y = \frac{4eU}{mr_0^2\omega^2} \tag{1}$$

$$q_x = -q_y = \frac{2eV}{mr_0^2\omega^2} \tag{2}$$

where U and V are the DC and alternating RF potential, respectively, ω is angular frequency of the applied RF, e is the electronic charge, m is the mass, r_0 is this distance from the z-axis (i.e. centre of the four rods) and a and q represent points in space. Plotting solutions of a and q against one another generates a graph defining the a and q values at which ions possess a stable trajectory through the quadrupole (Fig. 8).

Quadrupole mass analysers are advantageous as they are small, inexpensive, have a high scanning speed and when three are coupled together (triple quadrupole instrument) they are capable of selective reaction monitoring experiments (SRM). In a SRM experiment, Q1 and Q3 only allow transmission of a specified precursor and product ion, respectively, improving detection of a specific ion. On the other hand, they have a limited mass resolution and have a finite mass range unlike linear ToFs (Sect. 1.2.2.3) [76].

2.2.2 Quadrupole Ion Trap

Unlike quadrupole (and the later discussed ToF) mass analysers, quadrupole ion traps enable trapping and storage of gaseous ions that can be ejected after a defined

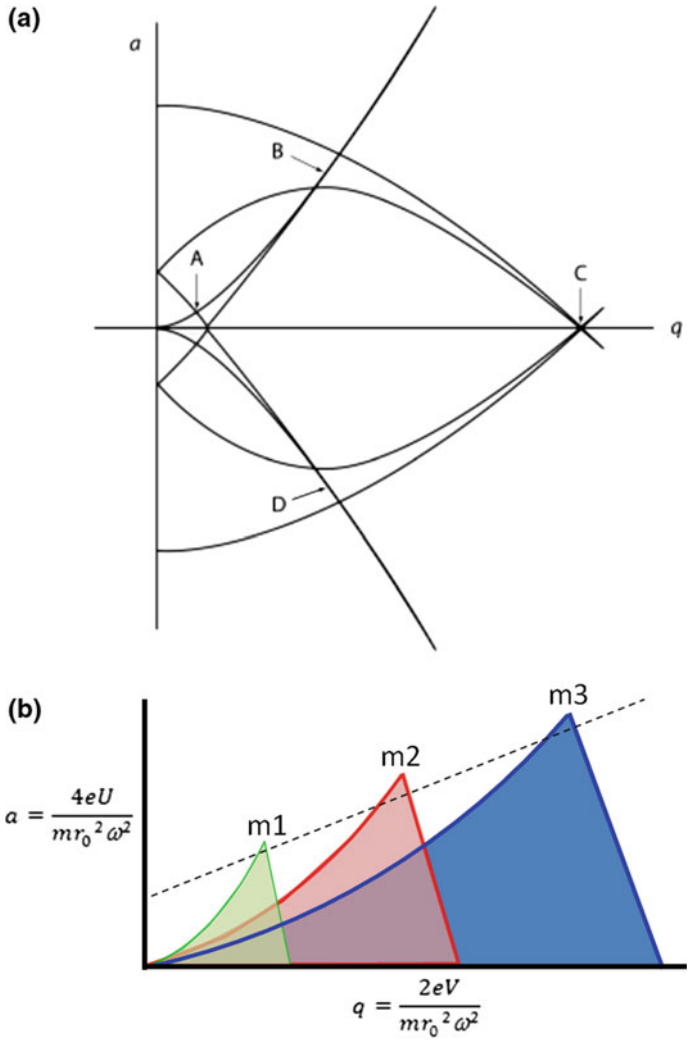

Fig. 8 Plot of solutions to the Mathieu equations for a given *m/z* (**a**). Regions highlighted as A, B, C and D are trajectories with both x and y stability. The majority of quadrupoles operate in stability region A (lower voltages) [77]. Also shown is a zoomed in diagram of region A for three ions with different *m/z,* (m1, m2 and m3) (*b*). The dashed line indicates the scan line for which trajectories for m1, m2 then m3 become stable as the magnitude of U:V is increased

period of time. For 3D quadrupole ion traps (Paul trap), ions are gated into the trap to prevent ion escape [65]. The trap itself consists of three hyperboloidal electrodes, two end-cap electrodes and a ring electrode between them (Fig. 9) [78]. DC and RF potentials are applied to the end-cap and ring electrodes, respectively, resulting in the formation of a parabolic potential well (shaped like a saddle in 3D), which ions

become trapped in [79]. Stable *m/z* ion trajectories are dictated by the Mathieu equations akin to quadrupoles (Fig. 8). An inert gas ($\sim$1 mTorr helium) is added to the trap to dampen the kinetic energy of the ions in the trap through collisions and as a result stabilises the ions trajectory and confines it to the centre of the trap. Ions can be ejected from the trap by linearly increasing the RF amplitude causing the ion trajectories to eventually become unstable, with low *m/z* becoming unstable first then higher *m/z*-ions, when the voltage reaches the resonant frequency of the ion, at which point the ions are ejected from the trap and are detected externally. Therefore, ions are not discarded prior to detection unlike beam type instruments [65]. RF voltages can also be applied to the end-cap electrodes in resonance with the periodicity for specific or multiple *m/z* ion(s), resulting in these trapped ions gaining kinetic energy and moving away from the centre of the trap. When this energy is high enough ions are ejected from the trap [78, 80]. This enables ejection of larger ions which would otherwise require impractically high voltages by raising the RF amplitude of the ring electrode alone [80]. Crucially, for tandem MS experiments, ions of a given *m/z* can also be isolated by this method. This resonance can also be exploited to raise the trapped ions kinetic energy enough so that they undergo CID without being ejected from the trap. This enables multiple ion dissociation stages to be performed (MS^n) [65, 80].

The main disadvantage of 3D ion traps is poor resolving power since small changes in the RF potential ramp can result in ejection of a 1 *m/z* window—under normal operating conditions 3D quadrupole ion traps can identify singly charged ions from *m/z* 500–2500 with a resolution of 0.2–0.5 Da [78]. They also have longer ion detection times given they trap ions for MS, as opposed to the μs required for ions to reach the detector from the source of beam type instruments.

Ions can also be trapped in linear quadrupole ion traps, which function in a similar manner to the 3D quadrupole ion traps except with elongation of all electrodes (additionally a buffer gas is not always essential for trapping). As a result, a greater number of ions can be trapped compared to the 3D ion traps. Furthermore, the ejection efficiency of linear quadrupole ion traps is much greater and therefore the sensitivity is improved [81]. However, the mass resolution is also much poorer and is typically limited to studying species *m/z* < 2000 [58]. It is also important for both types of ion traps to not overfill the trap, otherwise, space charge effects can become apparent, which will further reduce the resolving power and mass accuracy [81].

2.2.3 ToF

Linear and reflectron time-of-flight (ToF) mass analysers are capable of determining the *m/z* ratio of an ion from the time it takes that ion to travel through a field-free region in a vacuum after being accelerated by an electrical potential. Ions with lower *m/z* values reach the detector before those of high *m/z* values as they are accelerated to a greater velocity (v) [65]. This can be easily represented through equations for linear ToFs (linear drift region). The kinetic energy ($\frac{1}{2}mv^2$) gained by the ion is equal to the accelerating potential energy (eV where e is the charge of an

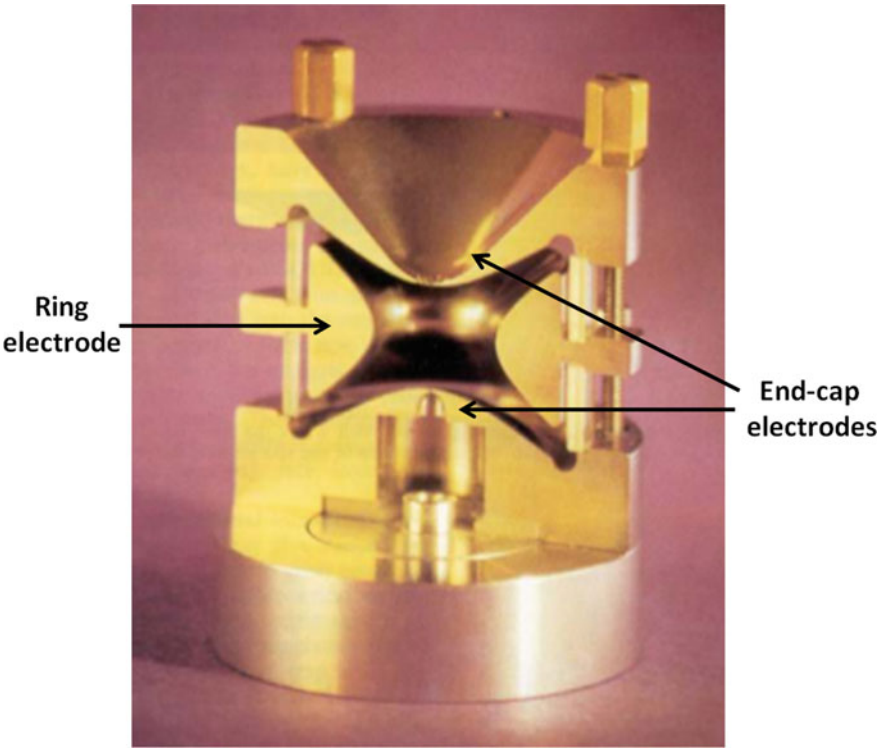

Fig. 9 Photograph of a transverse section of a 3D quadrupole ion trap with the electrodes labelled. Ions are trapped within the volume between the electrodes. Amended from March [78]

electron and V is the accelerating potential) (Eq. 3) and the time-of-flight (ToF) is related the length of the flight tube (L) (Eq. 4), the *m/z* value can thus be determined using Eq. 5 below:

$$zeV = \frac{1}{2}mv^2 \tag{3}$$

$$TOF = \frac{L}{v} \tag{4}$$

$$TOF = L\left(\frac{m}{2zeV}\right)^{\frac{1}{2}} \tag{5}$$

where z is the ion charge [58].

Reflectrons work around the same principle except that ions are reflected by an 'ion mirror' (*a* series of electrostatic ion guides with increasing potential) angled to reflect these ions towards a secondary detector preventing them from being reflected

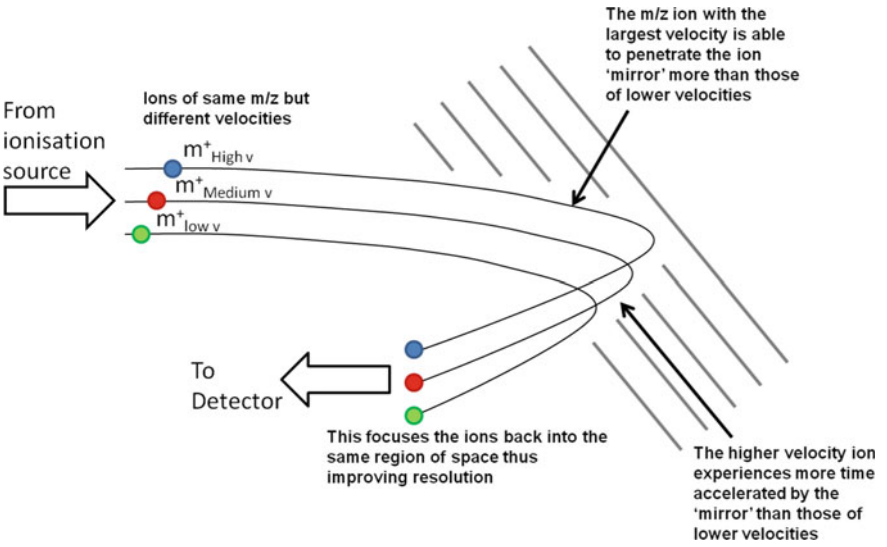

Fig. 10 Diagram depicting the reflectron mode ion trajectory for three ions, with identical *m/z* but different velocities, through a time-of-flight mass analyser

back to the source (Fig. 10) or colliding with other ions coming from the source. The purpose of the reflectron is to correct for differences in kinetic energy of ions of the same *m/z* value which would otherwise result in slight differences in computed mass and thus loss of resolution [82]. Ions of greater velocities penetrate into the reflectron 'mirror' more than those of a lower velocity. These ions are then accelerated towards the detector by the 'mirror'. The ions that had penetrated the mirror the most (higher kinetic energy) spends more time under an accelerating potential than the lower penetrating ions. This results in focussing the ions as the ones with a higher velocity have had to travel a longer distance. This v-optic reflectron is shown schematically in Fig. 10. A second reflection (w-optic) can increase the resolution even further, although this comes at the expense of sensitivity (factor of 3 compared to v-optic) as the longer drift-times increases the likelihood of metastable decomposition [58].

ToFs are advantageous as they can have a high resolving power and linear ToFs theoretically have no upper mass limit, as all that is required is the ion to be capable of travelling intact through the drift tube. Also spectra can be acquired rapidly, which allows for spectral averaging. However, reflectrons require a higher vacuum than quadrupole analyzers and the ambient temperature needs to be controlled very carefully so that the thermal energy of the ions is not increased [58]. MALDI ionisation is usually used in combination with a ToF mass analyser as they complement one another, since MALDI produces a defined pulse of ions allowing the packets time-of-flight to be measured. Also MALDI and the ToF analyser can be placed in-line reducing ion loss.

2.3 *Tandem Mass Spectrometry for the Analysis of Glycopeptides*

Fragmentation of (glyco)peptides can be used to determine the sequence of the peptide and also possibly the site that is glycosylated. There are three methods for fragmentation that shall be discussed, firstly collision-induced dissociation (CID), secondly electron transfer dissociation (ETD) and finally infrared multiphoton dissociation (IRMPD). There is a nomenclature for naming the ions produced by peptide and glycan fragmentation known as the Domon–Costello nomenclature (A-, B-, C-, X-, Y- and Z-ions) and the Roepstorff–Fohlmann–Biemann (a-, b-, c-, x-, y- and z-ions), respectively (Fig. 11) [51, 83].

2.3.1 CID

Collision-induced dissociation (CID) (previously referred to as collisionally activated dissociation or CAD) is the most common method used for fragmentation of glycans and peptides for sequence elucidation. For peptides, CID often generates b- and y-product ions derived from the *N*- and *C*-terminus, respectively, as a result of the amide bond dissociation (Fig. 11). CID of glycans (approximately 0.1–1 eV or 10–100 eV in ion trap or beam type analysers, respectively [84]) commonly results in fragmentation either side of the glycosidic bond generating B/C- and Z/Y-ions from the non-reducing and reducing termini, respectively. At higher energies, fragmentation across the ring is also observed. During CID, analyte ions are accelerated through

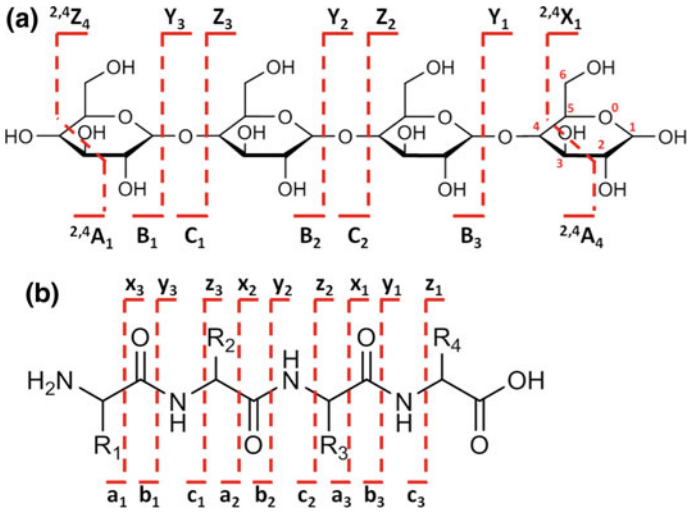

Fig. 11 Domon-Costello nomenclature for glycan fragmentation (**a**) [51] and Roepstorff-Fohlmann-Biemann nomenclature for peptide backbone fragmentation (**b**). [83]

an inert neutral gas such as helium or argon. The energy the analyte ion gains from colliding with the gas is converted into internal energy that is distributed throughout the structure. It results in dissociation of typically labile bonds although charge directed mechanisms may result in dissociation of thermodynamically more stable moieties. For protonated peptides, this charge directed cleavage is best described by the mobile proton model [85, 86]. The mobile proton model states that at high internal energy mobile protons are able to protonate less thermodynamically favourable positions, such as the amide nitrogen in the peptide backbone compared to when the internal energy is lower and protonates only basic residues. Protonation of the amide nitrogen weakens the bond and thus allows the peptide backbone to fragment [87]. Protonated glycoconjugates often fragment to yield primarily glycosidic product ions [88], whereas deprotonated species also generate cross-ring fragments [88–90]. However, since free-carbohydrates typically lack any basic groups (proton sinks), they often preferentially form metal adducts with sodium or potassium without an additional metal dopant. Doping carbohydrate samples with other metals such as lithium, silver [91], or manganese [92] greatly affects the propensity of specific product ions, which has been proposed to be a result of differential metal binding sites facilitating dissociation by differing pathways [92]. Typically, large ions with low charge densities, such as potassium and rubidium, tend to dissociate to lose the metal adduct over fragmenting the carbohydrate structure, whereas for small highly charged ions like lithium extensive fragmentation is observed [93–95]. At higher energies, cross-ring fragmentation also becomes prevalent compared to glycosidic fragmentation. Also the nature of glycosidic fragmentation depends on the metal adduct. It has been reported for example that $[M + Mg]^{2+}$ adducted carbohydrates dissociate to yield more cross-ring fragments compared to the $[M + 2Li]^{2+}$ equivalent, whilst $[M + Ag]^{+}$ adducts produce almost no cross-ring fragments [95]. Therefore, studying glycans and glycoconjugates with different adducts can produce complementary structural information [88, 96]. Additionally, chemical derivatization such as permethylation/acetylation appears to favour formation of glycosidic fragment ions [97]. Finally, the presence of other product ions depends on the identity of the glycan and its regiochemistry [98]. The stereochemistry of the glycosidic bond often results in different ion yields rather than the formation of different product ions. Currently, there is little knowledge of these product ion structures [51, 94, 99] and, unlike for peptides, no definitive mechanisms for glycan dissociation have been elucidated [85–87, 100, 101].

CID of glycoconjugates commonly yields diagnostic product ions losses such as *m/z* 162, 164, 180, 203 and 221 corresponding to dehydrated hexose, deoxy hexose, hexose, dehydrated *N*-acetylhexosamine and *N*-acetylhexosamine respectively. As a result, neutral loss scanning of these diagnostic species facilitates the identification of precursor glycoconjugates. Conversely, product ions analysis of glycan fragment ions (e.g. *m/z* 204 for $[HexNAc–H_2O + H]^{+}$) can also facilitate glycan precursor identification.

There are issues using CID fragmentation when studying glycans and their conjugates. Firstly, CID typically fragments the most labile bonds which for glycopeptides tend to be the glycosidic linkages between the peptide and the glycan

(although for high mannose containing *N*-glycans the glycosidic bond can remain intact). Loss of the glycan from *O*-glycopeptides goes via a mechanism that regenerates the alcohol group on the serine/threonine residues [102], preventing characterisation of the glycosylation site. This loss of the labile glycan moiety is elevated for beam instruments like quadrupole-ToFs [103]. Furthermore, this fragmentation pathway often comes at the expense of backbone fragmentation, therefore higher collisional energies are often required to fragment the peptide backbone [103]. In addition, the glycan chains themselves also fragment by CID typically producing B/Z- and C/Y-ions in positive ion mode, but A/X-ions can also be observed where the ring itself fragments greatly complicating tandem mass spectra [51]. CID-induced migrations of Fuc [104–106], hexose [107] and sulphate [108] groups have been observed for protonated and deprotonated carbohydrates, further complicating analysis [105, 107, 109, 110], although this has not yet been reported for metal adducted analytes [109, 111].

2.3.2 ETD

Electron transfer dissociation (ETD), not to be mistaken with electron capture dissociation (ECD), is a less widespread fragmentation technique compared to CID. Dissociation is achieved by an electron transfer reaction between a gaseous radical such as fluoranthene or anthracene and the analyte ions of interest. For peptides, the resultant radical ion is unstable and results in the fragmentation of the bond with the lowest barrier of dissociation, which tends to be the N–C_α backbone bond generating c- and z-ions (also fragmentation of the amine within proline has been reported) [112, 113]. ETD fragmentation is much more efficient for peptides with a high charge density as lower charge allows for the possibility of non-covalent intrapeptide interactions that could contain the extra electron, thus preventing dissociation [114]. Although overall fragmentation of smaller peptides by ETD is less efficient than CID, ETD has a major advantage as the glycosidic linkage does not preferentially undergo fragmentation thereby enabling the observation of fragment peptide ions with the glycan still attached [103]. Application of ETD, therefore, increases the likelihood of being able to pinpoint the site of glycosylation. However, for highly charged free glycans (such as glycosaminoglycans or high valency metal cations), ETD (and electron detachment dissociation) has been shown to be capable of causing primarily cross-ring fragmentation whereas CID produces primarily glycosidic dissociation [115–119].

2.3.3 IRMPD

Infrared multiphoton dissociation (IRMPD), first reported by Beauchamp and co-workers [120], involves irradiation of trapped mass-selected ions, typically achieved in quadrupole ion traps or Penning traps, with infrared radiation from a tunable infrared laser (Fig. 12). The wavelength of the laser is ramped over a period

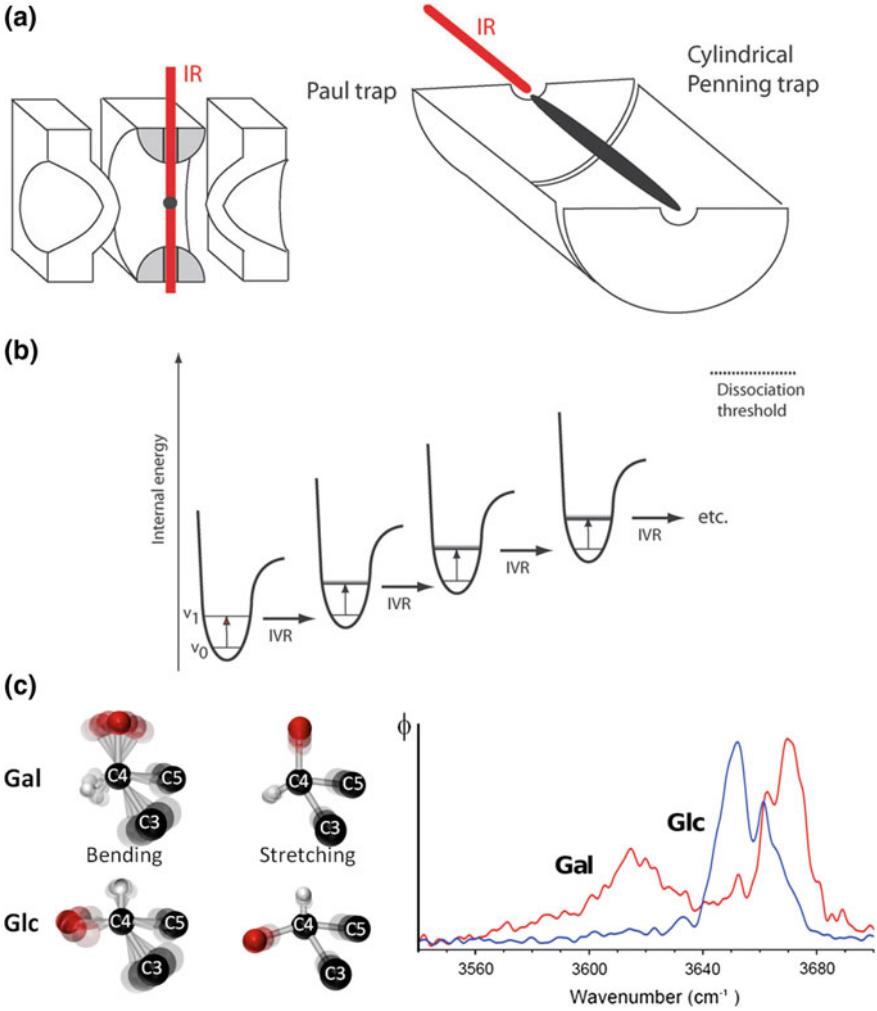

Fig. 12 Scheme depicting the typical orientation of the tuneable IR laser as it passes through the ion cloud in a Paul (3D-quadrupole ion) trap and Penning trap (**a**). Schematic of the IRMPD mechanism, the internal energy the ion gains resulting from photon absorption at the fundamental vibrational frequency is dissipated by sequential intramolecular vibrational re-distribution (IVR) events (**b**). Also depicted are cartoon bending and stretching modes for a region within hexose isomers Glc and Gal and the action IR spectra of these two molecules (**c**). Figure parts **a** and **c** are taken from Polfer [123]

of time causing unimolecular fragmentation (for carbohydrates this dissociation produces CID like product ions [121, 122]) of the trapped ions only when they possess resonant vibrational modes [123]. Therefore a plot of the wavelength against the fragmentation yield, ϕ, normalised to the respective laser power at each given frequency, generates an action IR spectrum of the gas-phase ion. Additional

molecular dynamic (MD) simulations can yield key atomistic or conformation information for small molecules or secondary structural features for peptides or proteins that would be unobtainable by convention MS-based methods alone [121–126]. Therefore IRMPD-MS could be an extremely powerful technique to aid characterisation of often isomeric carbohydrates [124, 126], though this approach is limited by the availability of bench top IR lasers that cover a wide and tunable range [123]. To achieve action IR spectroscopy spanning the majority of the IR range, free electron laser facilities are required [127]. Theoretical and experimental comparisons are also extremely challenging since theoretical calculations typically assume harmonic vibrational spectra, whereas experimental spectra are anharmonic. Also the absorption of IR radiation is not necessarily linearly scaled with the imparted energy, therefore experimental intensities may vary as compared to the theoretical spectra. Finally intramolecular vibrational re-distribution results in band broadening and red-shifting, which needs to be accounted for the experimental spectrum [123]. Generation of reasonable gas-phase candidate structures, from which theoretical IR spectra may be determined, is also not trivial given the typical inherent conformational diversity within molecules.

3 Glycan Sequencing Strategies

Glycan characterisation can be achieved to various degrees by a number of techniques. Most of these techniques are limited to studying solely glycan moieties that have been removed from their conjugates prior to characterisation, although methods exist that are capable of characterising the glycan constituents of intact glycoproteins [128], glycopeptides [46] or other glycosides [37, 129]. For *N*-glycans, glycan release is normally achieved enzymatically using one of three enzymes-peptide-*N*-glycosidase F (PNGase F), which selectively cleaves the bond between the reducing Glc*N*Ac residue and the Asn residue (preferably without a core α1-3 Fuc moiety); endoglycosidase F (Endo F) that cleaves between the chitobiose core; or endoglycosidase H (Endo H), which also cleaves between the chitobiose unit of only high mannose or hybrid *N*-glycans (Fig. 13) [2, 50]. As Endo F/H cleavage leaves a glycan unit attached to the protein/peptide, sites of glycosylation can also be characterised using typical proteomic strategies (e.g. proteolysis followed by LC-MS^2).

In comparison, the glycan moiety is completely removed when using PNGase F, also converting the Asn residue to Asp, making glycosite characterisation more challenging. This can be overcome by performing the transformation in ^{18}O-water which results in the formation of an ^{18}O-Asp residue [130]. No similar enzymes are known for *O*-glycan deglycosylation making them more challenging to process. As a result, *O*-glycans are typically cleaved chemically using either reductive β-elimination [48, 50, 131, 132] (Fig. 14) or hydrazinolysis (Fig. 15) [133–135]. However, hydrazinolysis may result in sequential loss of the reducing-terminal residues (peeling), inhibiting complete sequence elucidation [133, 134]. After

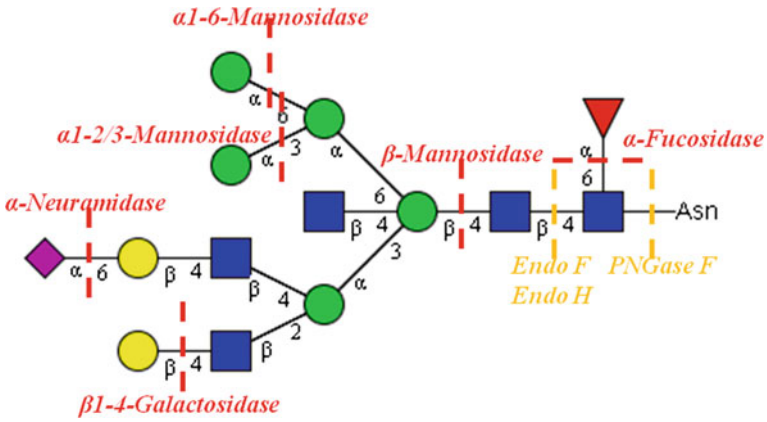

Fig. 13 Representative structure for a hybrid type *N*-glycan and the potential endoglycosidases (*orange*) and example exoglycosidases (*red*) that can act on it

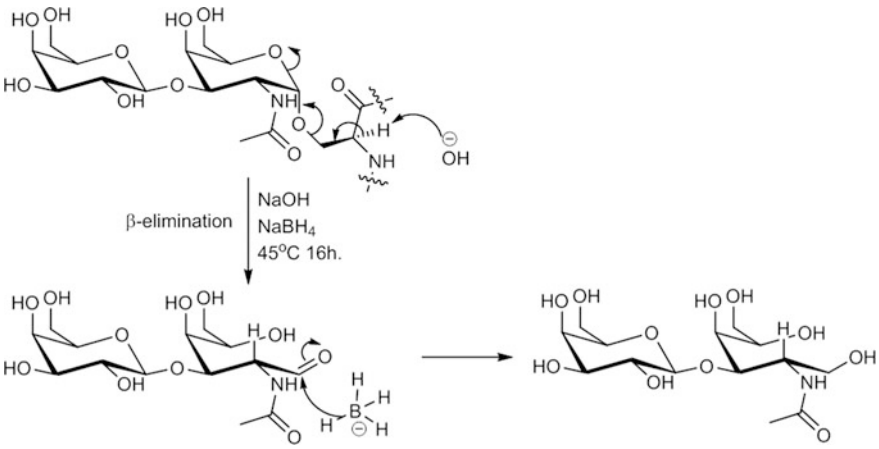

Fig. 14 Proposed mechanism for sodium borohydride induced reductive β-elimination of *O*-glycans [50]

release, the glycans can be enriched and purified using either lectin affinity [136–138], porous graphitised carbon (PGC) [139–141] or size exclusion columns [142] and/or tagged with a fluorescent label [49, 143, 144]. Since these glycans normally exist in multiple glycoforms, the released glycans are typically fractionated by chromatography prior to their characterisation [15, 145–149]. Conversely, glycans can be hydrolysed into their constituent monosaccharides by TFA or sulphuric acid treatment [150, 151] followed by re-*N*-acetylation [152]. The relative abundances and composition of these monosaccharides are then elucidated.

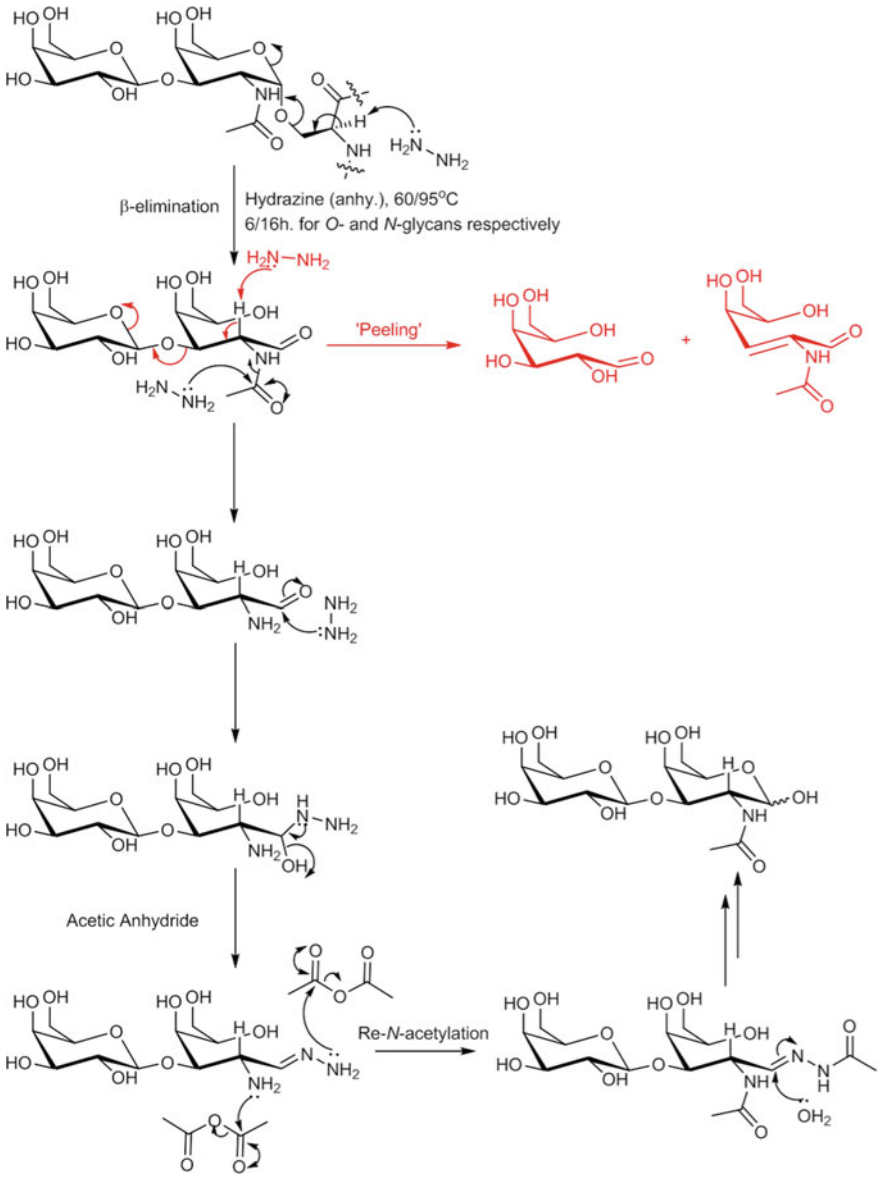

Fig. 15 Potential reaction mechanism for hydrazinolysis of an O-glycan including the 'Peeling' side reactions [135]

3.1 Glycosidase Treatment

Treatment of unknown glycans with cocktails of glycosidases, whose specificity and activity are well characterised, is one of the most routinely employed strategies to facilitate elucidating monosaccharide sequence and glycosidic linkage information [49, 50, 153]. Glycosidases fall into two groups, endoglycosidases that cleave non-terminal monosaccharides or glycosidic bonds to aglycons (such as proteins and lipids) and exoglycosidases that cleave monosaccharides from the non-reducing terminus in a stepwise manner. Both types are typically extremely specific for a given monosaccharide and linkage type. Therefore, sequential treatment of unknown glycans with specific exoglycosidases enables deduction of both the monosaccharide sequence and the linkage information. A wide variety of exoglycosidases have been characterised that cleave Galβ (Bovine testes) [154], Galβ1-4 (*Streptococcus pneumoniae*) [155], Glc*N*Acβ (*Streptococcus pneumoniae*) [156], Neu5Acα (*Streptococcus pneumoniae*) [157], Manα1-2/3 (*Xanthomonas manihotis*) [158], Manα1-6 (*Xanthomonas manihotis*) [158] and Fucα1-2 (*Xanthomonas manihotis*) [158] to name a few (Fig. 13). Detection of enzymatic hydrolysis products is facilitated by other analytical techniques (usually MS and/or LC) [15]. This approach is routinely employed in *N*-glycan sequencing. *N*-glycans consist of well-characterised core oligosaccharide structures and the enzymatic transformations that act on them all relatively well characterised (at least for mammalian systems) [15, 26, 153]. To enable characterisation, however, glycans must be purified prior to hydrolysis so that changes resulting from the enzymatic action can be monitored. Therefore, a priori fractionation techniques are required which can be challenging for oligosaccharides since they are often chemically similar. Additionally, glycosides capable of cleaving all potential glycosidic linkages have yet to be elucidated limiting this approach. Finally, the sequential enzymatic processes involved are low-throughput and often tedious [88].

3.2 Glycan-Binding Probes (GBPs)

One of the earliest approaches to identify carbohydrate structures was to employ well-characterised glycan-binding proteins (GBPs), such as lectins or antibodies, as affinity probes (Fig. 16) [138, 159–162]. A wide variety of GBP specificities has been characterised that recognise a diverse range of glycan moieties [20, 163–168]. This enables elucidation of a range of divergent carbohydrate functionalities. For example, the lectin Concanavalin A (ConA) preferably binds high mannose *N*-glycans (α-Man specific), whereas *Lotus tetragonolobus* lectin (LTL) binds to fucosylated glycans [163]. The difference in structural specificities of two GBPs can also be more subtle. For example, *Sambucus nigra* (SNA) only binds to α-2,6-sialylated carbohydrates [20], whereas *Maackia amurensis* II (MAL II) binds preferentially to terminal α-2,3-sialylated *N*-glycans [164]. Unlike most other

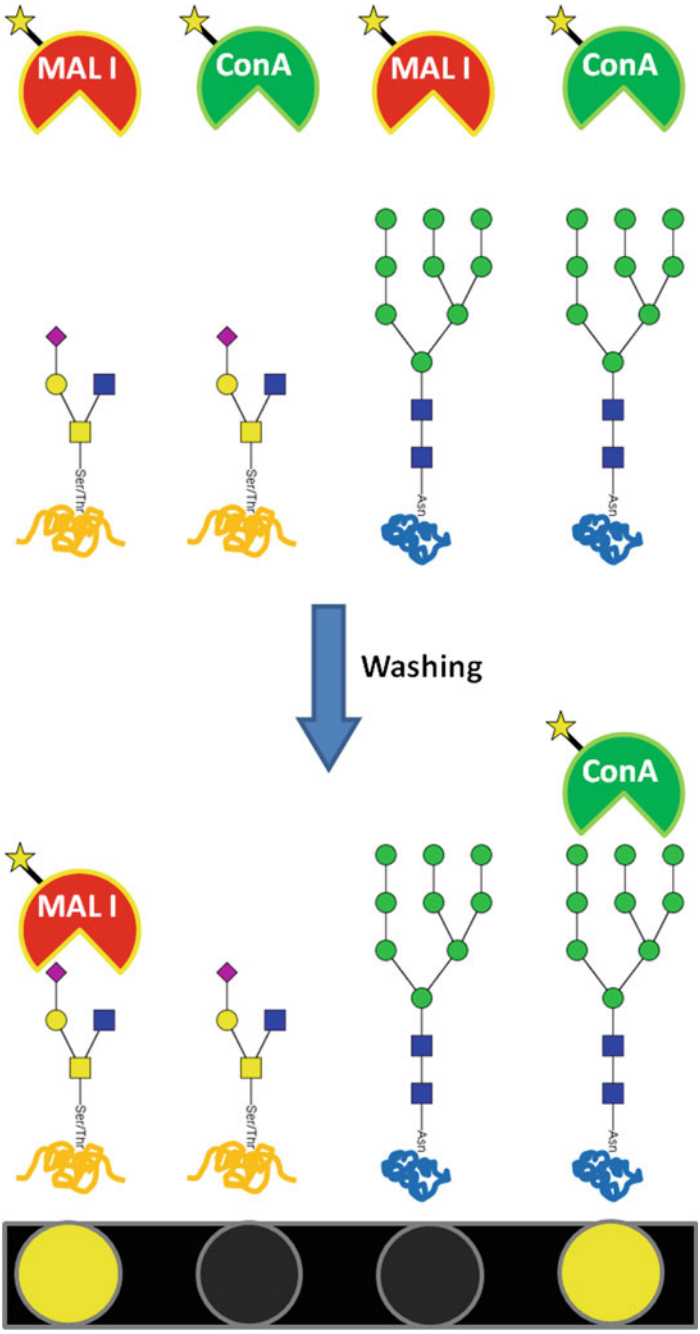

Fig. 16 Scheme depicting incubation of fluorescently tagged MAL I (sialic acid specific lectin) and ConA (high mannose *N*-glycan specific) with an array of *O*- and *N*-glycans and their resultant fluorescent response after washing

sequencing strategies, the use of GBPs allows for glycan profiling at the macroscopic level in the form of tissue staining [169, 170] and microscopic in the form of a cell [171, 172], as well as being capable of characterising glycoconjugates or free glycans [173–177]. These GBPs are typically labelled with a fluorescent or radioactive tags to facilitate detection of binding [138, 174, 178], which is disadvantageous compared to other label-free strategies, although label-free detections techniques are also viable in certain situations such as MALDI-ToF MS [161, 162] and surface plasmon resonance (SPR) spectroscopy [179, 180] can also be arrayed enabling high-throughput glycan profiling of glycoconjugates [36, 161, 162, 181–183] or even cells [172] and bacteria [184, 185]. Similarly, lectins can be attached to supports, enabling selective enrichment of glycosides with a given structural motif (lectin affinity chromatography) [186]. Unlike other profiling strategies, however, lectin arrays yield few molecular structural features and because of promiscuous lectin binding specificities, are liable to produce misleading information.

3.3 Liquid Chromatography

For carbohydrate analysis, liquid chromatography (LC) is exploited primarily as a separation and to a lesser extent as a characterisation tool [49, 50, 147, 187–190]. LC separates analytes based on their differing affinity towards a defined stationary phase. Analytes that display poor retention (or are highly soluble in the mobile phase) are sequentially eluted before those that have higher retention. Detection of eluted molecules is normally achieved by spectroscopic means if the analyte possess a chromophore or by MS when the LC is placed in-line with the mass spectrometer. Confirmation of an analytes identity can be facilitated through comparing its retention time to a known standard [188, 189]. This strategy has been greatly facilitated by the development of a database (GlycoBase) consisting of experimental chromatograms (and mass spectra) for various separation techniques (e.g. HPLC, capillary electrophoresis etc.) under a specified set of standard conditions [188, 189]. For glycans, monitoring alterations in glycan retention times (often described in ‘glucose units’ (GU) with reference to a ladder of dextran polymers [145]) after incubation with various glycosidase ‘cocktails’, whose specific activities are well characterised, can enable comprehensive elucidation of stereochemical sequences [15, 26, 37, 145]. This approach relies heavily on access to glycosidases capable of removing all natural glycosidic linkages, which currently is not achievable. Characterising unknown glycans with a series of glycosidases would also be time-consuming. LC techniques to separate carbohydrates have lagged behind other biomolecules, primarily because carbohydrates lack a distinct chromaphore to facilitate their detection [148]. Additionally, they display poor retention and separation on classical C_{18} reversed-phase (RP) columns given their highly hydrophilic nature [147, 191]. Recently, it has been reported though that separation of underivatized carbohydrates on RP columns can be improved through

incorporation of an orthogonal separation tools such as ion mobility-mass spectrometry (IM-MS) [147]. As a result of poor separation on RP columns, carbohydrates are typically derivatised prior to LC analysis to add a chromaphore and increase hydrophobicity. This is typically achieved through coupling of an aminated chromophore, such as 2-aminobenzamide, 2-aminobenzoic acid or 2-aminopyridine, to the reducing aldehyde functionality of carbohydrate moieties (reductive amination) [144, 192]. Permethylation of carbohydrates also improves retention on C_{18} RP-LC supports and facilitates MS-based detection [193, 194], although this relies on quantitative derivatization which can be challenging for larger sterically more hindered structures. Despite the application of these strategies, separation of glycan isomers remains challenging by C_{18} RP-LC methodology alone [148, 191, 195]. As a result several other LC approaches consisting of novel stationary phases have been developed, such as high pH (also referred to as high-performance) anion-exchange chromatography (HPAEC) [196], hydrophilic interaction chromatography (HILIC) [15, 197] and porous graphitic carbon (PGC) [140, 198, 199], which do not rely on derivatization strategies (Fig. 17).

HPAEC is well established for the high resolution separation of underivatized carbohydrates [196, 200, 201]. HPAEC columns typically consist of an agglomeration of non-porous polystyrene-divinylbenzene and smaller polystyrene-divinylbenzene beads possessing quaternary amine groups [200]. Carbohydrate samples are deprotonated with high pH mobile phases (pH > 12, linear gradient ~10–100 mM sodium hydroxide to sodium acetate) resulting in separation by anion-exchange with the quaternary amine stationary phase [200]. Classically glycans eluted from HPAEC columns are quantitatively detected by pulsed amperometric detection (PAD), since carbohydrate possess no chromophore.

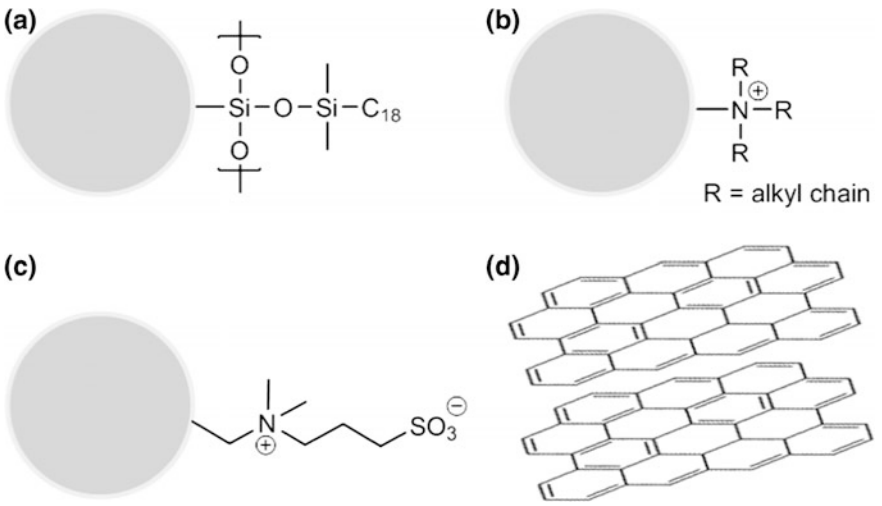

Fig. 17 Examples of common stationary phases for RP (C18) (**a**), HPAEC (CarboPac, dionex) (**b**), HILIC (ZIC-HILIC SeQuant®) (**c**) and PGC (**d**)

Conveniently, most of the eluted analyte can be recovered after detection. Unfortunately, HPAEC is often limited to small oligosaccharides (trisaccharides or less) and is thus typically used for monosaccharide composition analysis. Also due to the high-levels of salt, HPAEC is not amenable to MS-based analytical techniques without carbohydrate desalting [139]. HPAEC-PAD also requires a relatively large amount of analyte ($\sim$mg).

The separation mechanisms of HILIC chromatography are much more complex compared to RP and HPAEC [202] and are still not fully understood. The specific details of these mechanisms are beyond the scope of this chapter. HILIC employs polar stationary phases to which polar substrates are retained preferentially compared to the less-polar mobile phase (typically composed of acetonitrile). Polar carbohydrates are eluted by increasing the concentration of water within the mobile phase. This enables separation of a wide range of potentially isomeric carbohydrates including small oligosaccharides [203], *N*-glycans [15, 204] and glycopeptides [197]. Also unlike HPAEC, the mobile phase employed is compatible with label-free analytical techniques such as MS [204] and UV/Vis absorbance for oligosaccharides labelled with a chromaphore [15]. As a result, the use of HILIC separation within research science is rapidly growing [202].

PGC stationary phases are increasingly being employed for the desalting and separating underivatized carbohydrate samples [139, 140, 199, 204–206]. As separation of aqueous analytes occurs by both hydrophobic and electronic interactions with the PGC stationary phase, PGC chromatography is amenable to studying both polar and non-polar substrates [141]. The precise mechanisms associated with this separation behaviour are also poorly understood similar to HILIC [205]. Unlike most stationary phases, PGC is extraordinarily resilient to extreme operating conditions including pH 0–14, allowing separation of acidic and basic analytes in their neutral forms, respectively; and high temperatures (200 °C) that result in improved peak symmetry and potentially improved separation [207] and additionally accommodate for larger flow rates with little increase in back-pressure given the loss in viscosity associated with the mobile phase [205]. Like HILIC, PGC chromatography has been reported to be capable of separating branched and linear glycan regio- and stereoisomers [140, 198, 199, 208]. Few studies have been undertaken comparing PGC and HILIC, although a large study comparing 141 unique metabolites found HILIC (aminopropyl column at pH 9.45) provided the greatest separation of these species [209]. Estimation of PGC retention times from the glycan structure is also more challenging compared to HILIC and RP [204].

An issue for LC approaches for carbohydrate identification is that an internal standard is required to validate detected carbohydrates, although this requires a priori characterisation of that given structure for full structural elucidation [199]. Conversely, the retention times of a purified known reference library whose structures have been characterised can be compared to unknown structures. However, the isolation or synthesis of such a vast library would be extremely challenging given the challenges associated with their chemical synthesis [210, 211] and the huge number of potential structures glycans that can be formed from only a small subset of monosaccharide residues [212]. Finally, even with all these

LC methodologies, separation of certain glycan isomers remains a significant challenge [213], although this may be alleviated by using orthogonal tandem LC strategies [208].

3.4 Mass Spectrometry and Hyphenated Mass Spectrometry Methods

MS and tandem MS techniques are the most commonly employed approach to structurally characterise glycans or glycopeptides given their speed and sensitivity [88, 214, 215]. Additionally, unlike most of the other characterisation tools, mass spectrometry enables direct glycosite characterisation at the glycopeptide level.

However, the primary limitation associated with studying glycans by conventional MS approaches is that most of the common natural monosaccharide building blocks are simple epimers of one another and therefore possess identical *m/z* (Figs. 1 and 18). Therefore, MS alone, is limited to characterising the monosaccharide class (i.e. hexose, *N*-acetylhexosamine, deoxy hexose, etc.) and is insufficient to directly identify these monosaccharide units without the use of an orthogonal sequencing approach, and are (???) often achieved through characterising the glycan processing pathways [46]. Glycan regiochemistry and branching can be elucidated either from diagnostic fragment ions [98, 215, 216] or though analysis of tandem mass spectra of permethylated or peracetylated glycans, since glycosidic fragments will have a number methyl/acetyl groups equal to the number of branches from that residue [194]. However, incomplete peralkylation or peracetylation complicates identification of branching and they (????) often require an additional purification step *c.f.* their underivatized equivalents; although, as previously mentioned, peralkylation or peracetylation strategies are also advantageous as they improve chromatographic retention on classical RP columns and increases MS response [190, 194]. Peralkylation and peracetylation also increase the volatility and thermal stability of monosaccharides allowing their analysis by gas-chromatography MS [217]. Stereochemical assignment of the monosaccharide units and of the glycosidic bond linking them is much more challenging. As discussed previously in Sect. 1.3.1, shifts in *m/z* after application of specific well-characterised exoglycosidases allows for certain moieties to be elucidated depending on the availability of the exoglycosidase [218]. Spectral matching glycan [88, 98, 219–223] or glycopeptide [220, 224] experimental tandem mass spectra to those of synthesised reference standards have also shown promise in being able to discern stereochemical (and regiochemical) information. A drawback of spectral matching is the requirement of a characterised synthetic standard, which is not feasible for large oligosaccharides given the number of potential isomers and challenges associated with synthesising these standards. Although it is not clear how well spectral similarities observed for small oligosaccharide standards will extend to larger structures. Konda et al. have reported that MS^3 (???) of a diagnostic

fragment ion (*m/z* 221) corresponding to deprotonated Hex-glycolaldehyde produces a tandem mass spectrum that is diagnostic of the stereochemistry of the monosaccharide and anomeric configuration [215, 225]. This approach would require of a relatively small reference library to allow identification of all species, although the approach has currently only been developed on a relatively small reference library of Glc, Gal and Man. It also requires the formation of specific fragments that produce these MS^n structurally rich spectra, which may be challenging for larger structures. Further recent strategies include energy-resolved mass spectrometry (ER-MS), where the product ion yields are recorded against the specific collision energy imparted since different diastereoisomers may require different activation energies [226–230]. For carbohydrates, these approaches often require purification of glycan mixtures prior to analysis otherwise you are liable to record chimeric ER-MS of iso-bars/mers that cannot be readily deconvoluted. Using a variation of ER-MS, Nagy et al. reported the first separation of all natural aldohexose, ketohexose and pentose monosaccharide stereoisomers including enantiomers. This was achieved by initially forming diastereomeric complexes with the monosaccharide of interest, a chiral reference molecule (e.g. *L*-serine) and Cu^{2+}, fragmenting them by collision-induced dissociation (CID) at a specific energy and comparing the relative intensities of the product ions associated with loss of the chiral reference and the glycan (R_{fixed}) [228, 230]. However, this strategy cannot generate regio-/stereochemical information in regards to the glycosidic linkages and requires glycan hydrolysis to the monosaccharide species prior to analysis; the sequence in which the monosaccharides appear in the glycan cannot thus be determined directly. Combining ion mobility spectrometry, an orthogonal gas-phase separation technique, to ER-MS further improves discrimination of isomeric carbohydrates [229].

Ion mobility (IM) spectrometry is a growing technique to characterise or separate carbohydrates and is especially powerful when coupled to conventional MS and LC strategies. This recent surge in ion mobility analysis of glycans is primarily a result of the recent commercialisation of hybrid IM-MS instrumentation (2006).

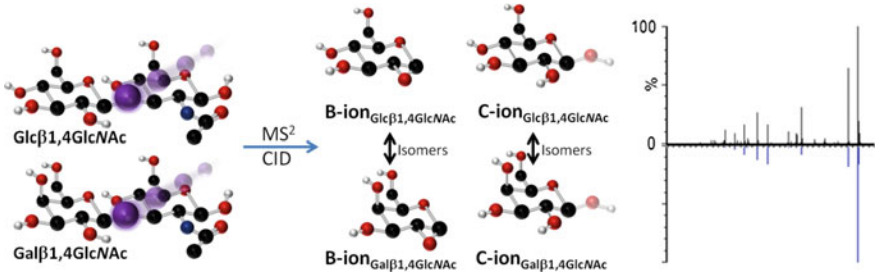

Fig. 18 Example of the spectral similarity within the tandem mass spectrum of two disaccharide isomers that have been fragmented by collision-induced dissociation (CID). Resulting product ions of these isomeric species are also isomers of one another. CID corresponds to collision-induced dissociation

IM separates species based on their rotationally averaged cross-sectional area-to-charge (Ω/z) ratio, a parameter that is intrinsic to a given molecule under a defined set of experimental conditions. Therefore, this technique possesses the capability of separating isomeric and isobaric glycan and glycoconjugates precursors and product ions, indistinguishable by MS alone and crucially when combined with molecular dynamics may facilitate elucidation of structural and conformational information [46, 129, 213, 229, 231–233].

Another drawback to using MS as an approach to characterise glycans is the reported rearrangement of glycan during CID of protonated carbohydrates, as previously mentioned in Sect. 1.2.3.1, making structure elucidation ambiguous [104, 109]. Although this migration has never been observed for metal cationised carbohydrates [109].

3.5 Alternative Approaches to Characterise Glycan Structures

NMR spectroscopy is currently the only analytical technique that can directly yield full three-dimensional structure and conformation elucidation of completely novel carbohydrates in solution [5, 234, 235]. Given the typical biological complexity of carbohydrates, 2D NMR experiments are normally acquired which improves spectral dispersion and can also yield important conformational information such as bond distances through-space between different or identical atoms for (Hetero) Nuclear Overhauser Effect spectroscopy (H/NOESY), respectively, and connectivity and stereochemical information for Heteronuclear Multiple-Quantum Correlation spectroscopy (HMQC) [5, 235], Correlation spectroscopy (COSY) [236] and Total Correlation spectroscopy (TOCSY) [46, 234]. The main disadvantages of NMR are that it is low-throughput, requires a relatively large amount of material which is typically not-amenable to biological samples and due to the spectra complexity of carbohydrates, samples need to be purified and isolated which is challenging for similar glycoforms. Additionally, spectra are normally extremely challenging to interpret and thus require computer assisted assignments [234].

X-ray crystallography also possesses the ability to give atomistic information on crystallised glycan and glycoconjugates structures [237, 238]. This technique like NMR is low-throughput and additionally requires regular crystals or carbohydrate structures, which underivatized carbohydrates rarely produce presumably due to their inherent flexibility. Additionally, due to their flexibility, carbohydrates tend to give poorly resolved crystal structures [237, 239].

4 Characterisation of Glycan-Binding Proteins

(Micro)array approaches are eminently suited for the elucidation of glycan-glycan-binding protein (GBP) partners as they can potentially offer the ability to screen >1000 reactions in a high-throughput manner [174] and require sub μL amounts of material. The application of array technology within both basic and applied (e.g. clinical) research science is highly diverse and has previously been used to study antigen binding [240], enzymatic transformations [175, 241, 242], bacterial binding [243] and glycan-GBP binding partners [138, 159, 174] to name a few. It is therefore unsurprising that there is a plethora of both array technologies and analytical techniques employed. A comprehensive list of array technologies and the analytical techniques used to screen them have been reviewed by us very recently [244]. Whilst this review focuses on the applications of array technologies to screen enzymatic transformations, the principles described in the review extend to studying substrate–ligand binding partners.

For applications immobilising glycans or GBPs to self-assembled monolayers (SAMs) on gold offer an ideal platform to study glycan–GBP partners. SAMs are relatively thermally and chemically stable and, to some extent, mimic the fluidity of the lipid bilayer motif present at the cell surface membrane [245]. These arrays can be screened directly by matrix-assisted laser desorption/ionisation (MALDI) time-of-flight (ToF) mass spectrometry (MS), a rapid label-free technique that reveals structural information on the bound analyte. When combined with routine bottom-up proteomics strategies, namely proteolytic digestion followed by MS and/or MS/MS of the generated peptides and subsequent database screening [246], the identity of unknown proteins can be determined [162, 179, 183]. Such arrays can, therefore, be utilised to characterise glycan-GBP partners directly from complex biofluids, without the need for a challenging labelling step as is often required for other common visualisation techniques such as fluorescence or radiation [138, 247].

5 Conclusions

Mass spectrometry-based methodologies have become key analytical tools both for carbohydrate sequencing and the characterisation of glycan-binding proteins. The key limitation of classical mass spectrometry as a ‘two-dimensional technique’ has been the lack of stereochemical information of glycan structure. Such shortcomings can be overcome by combining mass spectrometry with enzymatic digestion protocols and chromatographic techniques. Some very exciting recent developments are the adding of ion mobility spectrometry and IR spectroscopy in-line with mass spectrometry, used as hyphenated analytical techniques that give very high structural resolution.

References

1. Shin I, Park S, Lee MR (2005) Carbohydrate microarrays: An advanced technology for functional studies of glycans. Chem-Eur J 11:2894–2901
2. Varki A, C.R, Esko JD, et al. (2009) Essentials of glycobiology, 2 edn. Cold Spring Harbor, New York
3. Apweiler R, Hermjakob H, Sharon N (1999) On the frequency of protein glycosylation, as deduced from analysis of the SWISS-PROT database. Biochim Biophys Acta-Gen Subj 1473:4–8
4. Ohtsubo K, Marth JD (2006) Glycosylation in cellular mechanisms of health and disease. Cell 126:855–867
5. Yoshida-Moriguchi T et al (2010) O-Mannosyl phosphorylation of alpha-dystroglycan is required for laminin binding. Science 327:88–92
6. Sperandio M, Gleissner CA, Ley K (2009) Glycosylation in immune cell trafficking. Immunol Rev 230:97–113
7. Bode L (2012) Human milk oligosaccharides: every baby needs a sugar mama. Glycobiology
8. Poulin MB et al (2014) Specificity of a UDP-GalNAc pyranose-furanose mutase: a potential therapeutic target for campylobacter jejuni infections. ChemBioChem 15:47–56
9. Morris HR et al (1996) Gender-specific glycosylation of human glycodelin affects its contraceptive activity. J Biol Chem 271:32159–32167
10. Benoff S (1997) Carbohydrates and fertilization: an overview. Mol Hum Reprod 3:599–637
11. Schröter S, Osterhoff C, McArdle W, Ivell R (1999) The glycocalyx of the sperm surface. Human Reprod Update 5:302–313
12. Paszek MJ et al (2014) The cancer glycocalyx mechanically primes integrin-mediated growth and survival. Nat Adv Online Pub (2014)
13. Jacob F et al (2012) Serum antiglycan antibody detection of nonmucinous ovarian cancers by using a printed glycan array. Int J Cancer 130:138–146
14. Springer GFT, Tn (1984) General carcinoma auto-antigens. Science 224:1198–1206
15. Bones J, Mittermayr S, O'Donoghue N, Guttman A, Rudd PM (2010) Ultra performance liquid chromatographic profiling of serum N-glycans for fast and efficient identification of cancer associated alterations in glycosylation. Anal Chem 82:10208–10215
16. Chen YT et al (2013) Identification of novel tumor markers for oral squamous cell carcinoma using glycoproteomic analysis. Clin Chim Acta 420:45–53
17. Lauc G et al (2013) Loci associated with N-glycosylation of human immunoglobulin G show pleiotropy with autoimmune diseases and haematological cancers. PLoS Genet 9
18. Gornik O, Gornik I, Gasparovic V, Lauc G (2008) Change in transferrin sialylation is a potential prognostic marker for severity of acute pancreatitis. Clin Biochem 41:504–510
19. Hennet T (2012) Diseases of glycosylation beyond classical congenital disorders of glycosylation. Biochimica et Biophysica Acta (BBA)—General Subjects 1820:1306–1317
20. Iskratsch T, Braun A, Paschinger K, Wilson IBH (2009) Specificity analysis of lectins and antibodies using remodeled glycoproteins. Anal Biochem 386:133–146
21. Kumar SR, Sauter ER, Quinn TP, Deutscher SL (2005) Thomsen-friedenreich and Tn antigens in nipple fluid: carbohydrate biomarkers for breast cancer detection. Clin Cancer Res 11:6868–6871
22. Anthony RM et al (2008) Recapitulation of IVIG Anti-inflammatory activity with a recombinant IgG Fc. Science 320:373–376
23. Kanda Y et al (2007) Comparison of biological activity among nonfucosylated therapeutic IgG1 antibodies with three different N-linked Fc oligosaccharides: the high-mannose, hybrid, and complex types. Glycobiology 17:104–118
24. Thanabalasingham G et al (2013) Mutations in HNF1A result in marked alterations of plasma glycan profile. Diabetes 62:1329–1337
25. Lodish HF et al (2000) Molecular cell biology, 4th edn. New York

26. Royle L et al (2003) Secretory IgA N- and O-glycans provide a link between the innate and adaptive immune systems. J Biol Chem 278:20140–20153
27. Clardy J, Walsh C (2004) Lessons from natural molecules. Nature 432:829–837
28. Dalziel M, Crispin M, Scanlan CN, Zitzmann N, Dwek RA (2014) Emerging principles for the therapeutic exploitation of glycosylation. Science 343
29. Thaker MN, Wright GD (2015) Opportunities for synthetic biology in antibiotics: expanding glycopeptide chemical diversity. ACS Synth Biol 4:195–206
30. Ragauskas AJ et al (2006) The path forward for biofuels and biomaterials. Science 311:484–489
31. Azadi P, Inderwildi OR, Farnood R, King DA (2013) Liquid fuels, hydrogen and chemicals from lignin: a critical review. Renew Sust Energ Rev 21:506–523
32. Brinchi L, Cotana F, Fortunati E, Kenny JM (2013) Production of nanocrystalline cellulose from lignocellulosic biomass: technology and applications. Carbohydr Polym 94:154–169
33. Krištić J et al (2014) Glycans are a novel biomarker of chronological and biological ages. J Gerontol Series A: Biol Sci Med Sci 69:779–789
34. Wuhrer M et al (2006) Gender-specific expression of complex-type N-glycans in schistosomes. Glycobiology 16:991–1006
35. Krishnamoorthy L, Mahal LK (2009) Glycomic analysis: an array of technologies. ACS Chem Biol 4:715–732
36. Katrlik J, Svitel J, Gemeiner P, Kozar T, Tkac J (2010) Glycan and lectin microarrays for glycomics and medicinal applications. Med Res Rev 30:394–418
37. Marino K, Bones J, Kattla JJ, Rudd PM (2010) A systematic approach to protein glycosylation analysis: a path through the maze. Nat Chem Biol 6:713–723
38. Spiro RG (2002) Protein glycosylation: nature, distribution, enzymatic formation, and disease implications of glycopeptide bonds. Glycobiology 12:43R–56R
39. Mellquist JL, Kasturi L, Spitalnik SL, Shakin-Eshleman SH (1998) The amino acid following an asn-X-Ser/Thr sequon is an important determinant of N-linked core glycosylation efficiency. Biochemistry 37:6833–6837
40. Dell A, Galadari A, Sastre F, Hitchen P (2010) Similarities and differences in the glycosylation mechanisms in prokaryotes and eukaryotes. Int J Microbiol 2010:14
41. Mescher MF, Strominger JL (1976) Purification and characterization of a prokaryotic glucoprotein from the cell envelope of Halobacterium salinarium. J Biol Chem 251:2005–2014
42. Young NM et al (2002) Structure of the N-Linked glycan present on multiple glycoproteins in the gram-negative bacterium, Campylobacter jejuni. J Biol Chem 277:42530–42539
43. Stanley P (2011) Golgi glycosylation. Cold Spring Harbor Perspect. Biol 3
44. Roth Z, Yehezkel G, Khalaila I (2012) Identification and quantification of protein glycosylation. Int J Carbohydrate Chem 2012:10
45. Steentoft C et al (2013) Precision mapping of the human O-GalNAc glycoproteome through SimpleCell technology. The EMBO J 32:1478–1488
46. Both P et al (2014) Discrimination of epimeric glycans and glycopeptides using IM-MS and its potential for carbohydrate sequencing. Nat Chem 6:65–74
47. Hart GW, Copeland RJ (2010) Glycomics hits the big time. Cell 143:672–676
48. Jensen PH, Karlsson NG, Kolarich D, Packer NH (2012) Structural analysis of N- and O-glycans released from glycoproteins. Nat Protocols 7:1299–1310
49. Rudd PM et al (1997) Oligosaccharide sequencing technology. Nature 388:205–207
50. Morelle W, Michalski J-C (2007) Analysis of protein glycosylation by mass spectrometry. Nat Protocols 2:1585–1602
51. Domon B, Costello CE (1988) A systematic nomenclature for carbohydrate fragmentations in FAB-MS/MS spectra of glycoconjugates. Glycoconjugate J 5:397–409
52. Kebarle P, Verkerk UH (2009) Electrospray: from ions in solution to ions in the gas phase, what we know now. Mass Spectrom Rev 28:898–917
53. Ruotolo BT, Benesch JLP, Sandercock AM, Hyung SJ, Robinson CV (2008) Ion mobility-mass spectrometry analysis of large protein complexes. Nat Protoc 3:1139–1152

54. Hall Z, Politis A, Bush MF, Smith LJ, Robinson CV (2012) Charge-state dependent compaction and dissociation of protein complexes: insights from ion mobility and molecular dynamics. J Am Chem Soc 134:3429–3438
55. Mann M, Hendrickson RC, Pandey A (2001) Analysis of proteins and proteomes by mass spectrometry. Annu Rev Biochem 70:437–473
56. Konermann L, Ahadi E, Rodriguez AD, Vahidi S (2013) Unraveling the mechanism of electrospray ionization. Anal Chem 85:2–9
57. Liuni P, Wilson DJ (2011) Understanding and optimizing electrospray ionization techniques for proteomic analysis. Expert Rev Proteomics 8:197–209
58. Watson JT, Sparkman OD (2007) Introduction to mass spectrometry: instrumentation, applications and strategies for data interpretation. Wiley, New Jersey, 2007
59. Iribarne JV, Thomson BA (1976) Evaporation of small ions from charged droplets. J Chem Phys 64:2287–2294
60. Fernandez de la Mora J (2000) Electrospray ionization of large multiply charged species proceeds via Dole's charged residue mechanism. Anal Chim Acta 406:93–104
61. Yue XF, Vahidi S, Konermann L (2014) Insights into the mechanism of protein electrospray ionization from salt adduction measurements. J Am Soc Mass Spectrom 25:1322–1331
62. Chung JK, Consta S (2012) Release mechanisms of poly(ethylene glycol) macroions from aqueous charged nanodroplets. J Phys Chem B 116:5777–5785
63. Simpson RJ (2003) Proteins and proteomics: a laboratory manual. Cold Spring Harbor Laboratory Press, New York
64. Karas M, Gluckmann M, Schafer J (2000) Ionization in matrix-assisted laser desorption/ionization: singly charged molecular ions are the lucky survivors. J Mass Spectrom 35:1–12
65. Yates JR (1998) Mass spectrometry and the age of the proteome. J Mass Spectrom 33:1–19
66. El-Aneed A, Cohen A, Banoub J (2009) Mass Spectrometry, review of the basics: electrospray, MALDI, and commonly used mass analyzers. Appl Spectrosc Rev 44:210–230
67. Lewis JK, Wei J, Siuzdak G (2006) Encyclopedia of analytical chemistry. Wiley, New Jersey
68. Knochenmuss R (2013) MALDI ionization mechanisms: the coupled photophysical and chemical dynamics model correctly predicts 'temperature'-selected spectra. J Mass Spectrom 48:998–1004
69. Awad H, Khamis MM, El-Aneed A (2015) Mass spectrometry, review of the basics: ionization. Appl Spectrosc Rev 50:158–175
70. Knochenmuss R (2006) Ion formation mechanisms in UV-MALDI. Analyst 131:966–986
71. Karas M, Kruger R (2003) Ion formation in MALDI: the cluster ionization mechanism. Chem Rev 103:427–439
72. Ehring H, Karas M, Hillenkamp F (1992) Role of photoionization and photochemistry in ionization processes of organic-molecules and relevance for matrix-assisted lader desorption ionization mass-spectrometry. Org Mass Spectrom 27:472–480
73. Jaskolla TW, Karas M (2011) Compelling evidence for lucky survivor and gas phase protonation: the unified MALDI analyte protonation mechanism. J Am Soc Mass Spectrom 22:976–988
74. Batoy S, Akhmetova E, Miladinovic S, Smeal J, Wilkins CL (2008) Developments in MALDI mass spectrometry: the quest for the perfect matrix. Appl Spectrosc Rev 43:485–550
75. Miller PE, Denton MB (1986) The quadrupole mass filter—basic operating concepts. J Chem Educ 63:617–622
76. Shaw LM, Kwong TC (2001) The clinical toxicology laboratory: contemporary practice of poisoning evaluation. American Association for Clinical Chemistry, Incorporated, USA
77. Barner-Kowollik C, Gruendling T, Falkenhagen J, Weidner S (2012) Mass spectrometry in polymer chemistry. Wiley, New Jersey
78. March RE (1997) An introduction to quadrupole ion trap mass spectrometry. J Mass Spectrom 32:351–369

79. Jonscher KR, Yates Iii JR (1997) The quadrupole ion trap mass spectrometer—a small solution to a big challenge. *Anal. Biochem.* 244:1–15
80. Payne AH, Glish GL (2005) In: Methods in enzymology, vol 402, Academic Press, pp 109–148
81. Douglas DJ, Frank AJ, Mao DM (2005) Linear ion traps in mass spectrometry. Mass Spectrom Rev 24:1–29
82. Wiley WC, McLaren IH (1955) Time-of-flight mass spectrometer with improved resolution. Rev Sci Instrum 26:1150–1157
83. Roepstorff P, Fohlman J (1984) Proposal for a common nomenclature for sequence ions in mass-spectra of peptides. Biomedical Mass Spectrometry 11:601–601
84. Dodds ED (2012) Gas-phase dissociation of glycosylated peptide ions. Mass Spectrom Rev 31:666–682
85. Dongré AR, Jones JL, Somogyi Á, Wysocki VH (1996) Influence of peptide composition, gas-phase basicity, and chemical modification on fragmentation efficiency: evidence for the mobile proton model. J Am Chem Soc 118:8365–8374
86. Burlet O, Orkiszewski RS, Ballard KD, Gaskell SJ (1992) Charge promotion of low-energy fragmentations of peptide ions. Rapid Commun Mass Spectrom 6:658–662
87. Paizs B, Suhai S (2005) Fragmentation pathways of protonated peptides. Mass Spectrom Rev 24:508–548
88. Chen XY, Flynn GC (2009) Gas-phase oligosaccharide nonreducing end (GONE) sequencing and structural analysis by reversed phase hplc/mass spectrometry with polarity switching. J Am Soc Mass Spectrom 20:1821–1833
89. Domann P, Spencer DIR, Harvey DJ (2012) Production and fragmentation of negative ions from neutral N-linked carbohydrates ionized by matrix-assisted laser desorption/ionization. Rapid Commun Mass Spectrom 26:469–479
90. Zaia J, Miller MJC, Seymour JL, Costello CE (2007) The role of mobile protons in negative ion CID of oligosaccharides. J Am Soc Mass Spectrom 18:952–960
91. Harvey DJ (2005) Ionization and fragmentation of N-linked glycans as silver adducts by electrospray mass spectrometry. Rapid Commun Mass Spectrom 19:484–492
92. Zhu F, Glover M, Shi H, Trinidad J, Clemmer D (2015) Populations of metal-glycan structures influence MS fragmentation patterns. J Am Soc Mass Spectrom 26:25–35
93. Cancilla MT, Penn SG, Carroll JA, Lebrilla CB (1996) Coordination of alkali metals to oligosaccharides dictates fragmentation behavior in matrix assisted laser desorption ionization/Fourier transform mass spectrometry. J Am Chem Soc 118:6736–6745
94. Cancilla MT, Wang AW, Voss LR, Lebrilla CB (1999) Fragmentation reactions in the mass spectrometry analysis of neutral oligosaccharides. Anal Chem 71:3206–3218
95. Zaia J (2004) Mass spectrometry of oligosaccharides. Mass Spectrom Rev 23:161–227
96. Deguchi K et al (2006) Complementary structural information of positive- and negative-ion MSn spectra of glycopeptides with neutral and sialylated N-glycans. Rapid Commun Mass Spectrom 20:741–746
97. Domon B, Mueller DR, Richter WJ (1994) Tandem mass-spectrometric analysis of fixed-charge derivatized oligosaccharides. Org Mass Spectrom 29:713–719
98. Azenha CSR, Coimbra MA, Moreira ASP, Domingues P, Domingues MRM (2013) Differentiation of isomeric β-(1–4) hexose disaccharides by positive electrospray tandem mass spectrometry. J Mass Spectrom 48:548–552
99. Brown DJ et al (2011) Direct evidence for the ring opening of monosaccharide anions in the gas phase: photodissociation of aldohexoses and aldohexoses derived from disaccharides using variable-wavelength infrared irradiation in the carbonyl stretch region. Carbohydr Res 346:2469–2481
100. Polfer NC, Bohrer BC, Plasencia MD, Paizs B, Clemmer DE (2008) On the dynamics of fragment isomerization in collision-induced dissociation of peptides. J Phys Chem A 112:1286–1293

101. Riba-Garcia I, Giles K, Bateman RH, Gaskell SJ (2008) Evidence for structural variants of a- and b-type peptide fragment ions using combined ion mobility/mass spectrometry. J Am Soc Mass Spectrom 19:609–613
102. Darula Z, Chalkley RJ, Baker P, Burlingame AL, Medzihradszky KF (2010) Mass spectrometric analysis, automated identification and complete annotation of O-linked glycopeptides. Eur J Mass Spectrom 16:421–428
103. Zaia J (2010) Mass Spectrometry and Glycomics. Omics 14:401–418
104. Franz AH, Lebrilla CB (2002) Evidence for long-range glycosyl transfer reactions in the gas phase. J Am Soc Mass Spectrom 13:325–337
105. Harvey DJ et al (2002) "Internal residue loss": Rearrangements occurring during the fragmentation of carbohydrates derivatized at the reducing terminus. Anal Chem 74:734–740
106. Wuhrer M, Koeleman CAM, Hokke CH, Deelder AM (2006) Mass spectrometry of proton adducts of fucosylated N-glycans: fucose transfer between antennae gives rise to misleading fragments. Rapid Commun Mass Spectrom 20:1747–1754
107. Wuhrer M, Koeleman CAM, Deelder AM (2009) Hexose rearrangements upon fragmentation of N-glycopeptides and reductively aminated N-glycans. Anal Chem 81:4422–4432
108. Kenny DT, Issa SMA, Karlsson NG (2011) Sulfate migration in oligosaccharides induced by negative ion mode ion trap collision-induced dissociation. Rapid Commun Mass Spectrom 25:2611–2618
109. Wuhrer M, Deelder AM, van der Burgt YEM (2011) Mass spectrometric glycan rearrangements. Mass Spectrom Rev 30:664–680
110. Brull LP et al (1997) Loss of internal 1-> 6 substituted monosaccharide residues from underivatized and per-O-methylated trisaccharides. J Am Soc Mass Spectrom 8:43–49
111. Brüll LP, Kovácik V, Thomas-Oates JE, Heerma W, Haverkamp J (1998) Sodium-cationized oligosaccharides do not appear to undergo 'internal residue loss' rearrangement processes on tandem mass spectrometry. Rapid Commun Mass Spectrom 12:1520–1532
112. Chi A et al (2007) Analysis of phosphorylation sites on proteins from Saccharomyces cerevisiae by electron transfer dissociation (ETD) mass spectrometry. Proc. Natl. Acad. Sci. USA. 104:2193–2198
113. Syka JEP, Coon JJ, Schroeder MJ, Shabanowitz J, Hunt DF (2004) Peptide and protein sequence analysis by electron transfer dissociation mass spectrometry. Proc. Natl. Acad. Sci. USA. 101:9528–9533
114. Molina H, Horn DM, Tang N, Mathivanan S, Pandey A (2007) Global proteomic profiling of phosphopeptides using electron transfer dissociation tandem mass spectrometry. Proc. Natl. Acad. Sci. USA 104:2199–2204
115. Han L, Costello C (2011) Electron transfer dissociation of milk oligosaccharides. J Am Soc Mass Spectrom 22:997–1013
116. Leach FE III et al (2012) Hexuronic Acid stereochemistry determination in chondroitin sulfate glycosaminoglycan oligosaccharides by electron detachment dissociation. J Am Soc Mass Spectrom 23:1488–1497
117. Leach FE III et al (2011) Negative electron transfer dissociation Fourier transform mass spectrometry of glycosaminoglycan carbohydrates. Eur J Mass Spectrom 17:167–176
118. Wolff JJ et al (2010) Negative electron transfer dissociation of glycosaminoglycans. Anal Chem 82:3460–3466
119. Wolff JJ, Chi L, Linhardt RJ, Amster IJ (2007) Distinguishing glucuronic from iduronic acid in glycosaminoglycan tetrasaccharides by using electron detachment dissociation. Anal Chem 79:2015–2022
120. Woodin RL, Bomse DS, Beauchamp JL (1978) Multi-photon dissociation of molecules with low-power continuous wave infrared-laser radiation. J Am Chem Soc 100:3248–3250
121. Polfer NC et al (2006) Differentiation of isomers by wavelength-tunable infrared multiple-photon dissociation-mass spectrometry: application to glucose-containing disaccharides. Anal Chem 78:670–679

122. Stefan SE, Eyler JR (2010) Differentiation of glucose-containing disaccharides by infrared multiple photon dissociation with a tunable CO2 laser and Fourier transform ion cyclotron resonance mass spectrometry. Int J Mass Spectrom 297:96–101
123. Polfer NC (2011) Infrared multiple photon dissociation spectroscopy of trapped ions. Chem Soc Rev 40:2211–2221
124. Schindler B et al (2014) Distinguishing isobaric phosphated and sulfated carbohydrates by coupling of mass spectrometry with gas phase vibrational spectroscopy. Phys Chem Chem Phys 16:22131–22138
125. Barnes L et al (2015) Anharmonic simulations of the vibrational spectrum of sulfated compounds: application to the glycosaminoglycan fragment glucosamine 6-sulfate. Phys. Chem. Chem, Phys
126. Tan Y, Polfer N (2015) Linkage and anomeric differentiation in trisaccharides by sequential fragmentation and variable-wavelength infrared photodissociation. J Am Soc Mass Spectrom 26:359–368
127. Oepts D, van der Meer AFG, van Amersfoort PW (1995) The free-electron-laser user facility FELIX. Infrared Phys Technol 36:297–308
128. Wang H et al (2014) Multiplex profiling of glycoproteins using a novel bead-based lectin array. Proteomics 14:78–86
129. Pičmanová M et al (2015) A recycling pathway for cyanogenic glycosides evidenced by the comparative metabolic profiling in three cyanogenic plant species. Biochem J 469:375–389
130. Gonzalez J et al (1992) A method for determination of N-glycosylation sites in glycoproteins by collision-induced dissociation analysis in fast atom bombardment mass spectrometry: Identification of the positions of carbohydrate-linked asparagine in recombinant α-amylase by treatment with peptide-N-glycosidase F in 18O-labeled water. Anal Biochem 205:151–158
131. Duk M, Ugorski M, Lisowska E (1997) β-Elimination of O-glycans from glycoproteins transferred to immobilon P membranes: method and some applications. Anal Biochem 253:98–102
132. Stalnaker SH et al (2010) Site mapping and characterization of O-glycan structures on α-dystroglycan Isolated from rabbit skeletal muscle. J Biol Chem 285:24882–24891
133. Patel T et al (1993) Use of hydrazine to release in intact and unreduced form both N-linked and O-linked oligosaccharides from glycoproteins. Biochemistry 32:679–693
134. Kozak RP, Royle L, Gardner RA, Fernandes DL, Wuhrer M (2012) Suppression of peeling during the release of O-glycans by hydrazinolysis. Anal Biochem 423:119–128
135. Merry AH et al (2002) Recovery of Intact 2-aminobenzamide-labeled O-glycans released from glycoproteins by hydrazinolysis. Anal Biochem 304:91–99
136. Choi E, Loo D, Dennis JW, O'Leary CA, Hill MM (2011) High-throughput lectin magnetic bead array-coupled tandem mass spectrometry for glycoprotein biomarker discovery. Electrophoresis 32:3564–3575
137. Angeloni S et al (2005) Glycoprofiling with micro-arrays of glycoconjugates and lectins. Glycobiology 15:31–41
138. Kuno A et al (2005) Evanescent-field fluorescence-assisted lectin microarray: a new strategy for glycan profiling. Nat Methods 2:851–856
139. Packer N, Lawson M, Jardine D, Redmond J (1998) A general approach to desalting oligosaccharides released from glycoproteins. Glycoconjugate J. 15:737–747
140. Itoh S et al (2002) Simultaneous microanalysis of N-linked oligosaccharides in a glycoprotein using microbore graphitized carbon column liquid chromatography-mass spectrometry. J Chromatogr A 968:89–100
141. Hennion M-C (2000) Graphitized carbons for solid-phase extraction. J Chromatogr A 885:73–95
142. Powell AK, Ahmed YA, Yates EA, Turnbull JE (2010) Generating heparan sulfate saccharide libraries for glycomics applications. Nat Protoc 5:821–833
143. Harvey DJ (2000) Electrospray mass spectrometry and fragmentation of N-linked carbohydrates derivatized at the reducing terminus. J Am Soc Mass Spectrom 11:900–915

144. Bigge JC et al (1995) Nonselective and efficient fluorescent labeling of glycans using 2-amino benzamide and anthranilic acid. Anal Biochem 230:229–238
145. Guile GR, Rudd PM, Wing DR, Prime SB, Dwek RA (1996) A rapid high-resolution high-performance liquid chromatographic method for separating glycan mixtures and analyzing oligosaccharide profiles. Anal Biochem 240:210–226
146. Takegawa Y et al (2006) Simple separation of isomeric sialylated N-glycopeptides by a zwitterionic type of hydrophilic interaction chromatography. J Sep Sci 29:2533–2540
147. Lareau NM, May JC, McLean JA (2015) Non-derivatized glycan analysis by reverse phase liquid chromatography and ion mobility-mass spectrometry. The Analyst 140:3335–3338
148. Alley WR, Mann BF, Novotny MV (2013) High-sensitivity analytical approaches for the structural characterization of glycoproteins. Chem Rev 113:2668–2732
149. Stadlmann J, Pabst M, Kolarich D, Kunert R, Altmann F (2008) Analysis of immunoglobulin glycosylation by LC-ESI-MS of glycopeptides and oligosaccharides. Proteomics 8:2858–2871
150. Lohmander LS (1986) Analysis by high-performance liquid chromatography of radioactively labeled carbohydrate components of proteoglycans. Anal Biochem 154:75–84
151. Pettolino FA, Walsh C, Fincher GB, Bacic A (2012) Determining the polysaccharide composition of plant cell walls. Nat. Protocols 7:1590–1607
152. Byers HL, Tarelli E, Homer KA, Beighton D (1999) Sequential deglycosylation and utilization of the N-linked, complex-type glycans of human a1-acid glycoprotein mediates growth of Streptococcus oralis. Glycobiology 9:469–479
153. Kannicht C, Grunow D, Lucka L (2008) In: Kannicht C (ed) Post-translational modifications of proteins, Vol 446, pp 255–266. Humana Press
154. Distler JJ, Jourdian GW (1973) The purification and properties of β-galactosidase from bovine testes. J Biol Chem 248:6772–6780
155. Zahner D, Hakenbeck R (2000) The Streptococcus pneumoniae beta-galactosidase is a surface protein. J Bacteriol 182:5919–5921
156. Clarke VA, Platt N, Butters TD (1995) Cloning and expression of the β-N-acetylglucosaminidase gene from Streptococcus pneumoniae: generation of truncated enzymes with modified aglycon specificity. J Biol Chem 270:8805–8814
157. Camara M, Boulnois GJ, Andrew PW, Mitchell TJ (1994) A neuraminidase from Streptococcus-pneumoniae was the features of surface protein. Infect Immun 62:3688–3695
158. Wongmadden ST, Landry D (1995) Purification and characterization of novel glycosidases from the bacterial genus Xanthomonas. Glycobiology 5:19–28
159. Pilobello KT, Krishnamoorthy L, Slawek D, Mahal LK (2005) Development of a lectin microarray for the rapid analysis of protein glycopatterns. ChemBioChem 6:985–989
160. Zheng T, Peelen D, Smith LM (2005) Lectin arrays for profiling cell surface carbohydrate expression. J Am Chem Soc 127:9982–9983
161. Hu S, Wong DT (2009) Lectin microarray. Proteom. Clin. Appl. 3:148–154
162. Beloqui A et al (2013) Analysis of Microarrays by MALDI-TOF MS. Angew Chem Int Ed 52:7477–7481
163. Debray H, Decout D, Strecker G, Spik G, Montreuil J (1981) Specificity of 12 lectins towards oligosaccharides and glycopeptides relted to N-glycosylproteins. Eur J Biochem 117:41–55
164. Geisler C, Jarvis DL (2011) Letter to the Glyco-Forum: Effective glycoanalysis with Maackia amurensis lectins requires a clear understanding of their binding specificities. Glycobiology 21:988–993
165. Porter A et al (2010) A motif-based analysis of glycan array data to determine the specificities of glycan-binding proteins. Glycobiology 20:369–380
166. Yan LY et al (1997) Immobilized Lotus tetragonolobus agglutinin binds oligosaccharides containing the Le(x) determinant. Glycoconjugate J 14:45–55
167. Kletter D, Singh S, Bern M, Haab BB (2013) Global Comparisons of Lectin-Glycan Interactions Using a Database of Analyzed Glycan Array Data. Mol Cell Proteomics 12:1026–1035

168. Consortium for Functional Glycomics, http://www.functionalglycomics.org/. (2001)
169. Akimoto Y, Kawakami H (2014) In: Hirabayashi J (ed) Lectins, Vol. 1200, pp 153–163. Springer, New York
170. Mannoji H, Yeger H, Becker LE (1986) A specific histochemical marker (lectin Ricinus-communis agglutinin-1) for normal human microglia, and apllication to routine histopathology. Acta Neuropathol 71:341–343
171. Landemarre L, Cancellieri P, Duverger E (2013) Cell surface lectin array: parameters affecting cell glycan signature. Glycoconjugate J. 30:195–203
172. Nishijima Y et al (2012) Glycan profiling of endometrial cancers using lectin microarray. Genes Cells 17:826–836
173. Furukawa J-I et al (2008) Comprehensive Approach to Structural and Functional Glycomics Based on Chemoselective Glycoblotting and Sequential Tag Conversion. Anal Chem 80:1094–1101
174. Blixt O et al (2004) Printed covalent glycan array for ligand profiling of diverse glycan binding proteins. Proc. Natl. Acad. Sci. U S A 101:17033–17038
175. Blixt O et al (2008) Glycan microarrays for screening sialyltransferase specificities. Glycoconjugate J. 25:59–68
176. Blixt O et al (2010) A high-throughput O-glycopeptide discovery platform for seromic profiling. J Proteome Res 9:5250–5261
177. Ban L et al (2012) Discovery of glycosyltransferases using carbohydrate arrays and mass spectrometry. Nat Chem Biol 8:769–773
178. Paulson JC, Blixt O, Collins BE (2006) Sweet spots in functional glycomics. Nat Chem Biol 2:238–248
179. Remy-Martin F et al (2012) Surface plasmon resonance imaging in arrays coupled with mass spectrometry (SUPRA–MS): proof of concept of on-chip characterization of a potential breast cancer marker in human plasma. Anal Bioanal Chem 404:423–432
180. Munoz FJ et al (2009) Glycan tagging to produce bioactive ligands for a surface plasmon resonance (SPR) study via immobilization on different surfaces. Bioconjugate Chem. 20:673–682
181. Etxebarria J, Calvo J, Martin-Lomas M, Reichardt NC (2012) Lectin-array blotting: profiling protein glycosylation in complex mixtures. ACS Chem Biol 7:1729–1737
182. Koshi Y, Nakata E, Yamane H, Hamachi I (2006) A fluorescent lectin array using supramolecular hydrogel for simple detection and pattern profiling for various glycoconjugates. J Am Chem Soc 128:10413–10422
183. Li C et al (2009) Pancreatic cancer serum detection using a lectin/glyco-antibody array method. J Proteome Res 8:483–492
184. Hsu K-L, Mahal LK (2006) A lectin microarray approach for the rapid analysis of bacterial glycans. Nat. Protocols 1:543–549
185. Hsu KL, Pilobello KT, Mahal LK (2006) Analyzing the dynamic bacterial glycome with a lectin microarray approach. Nat Chem Biol 2:153–157
186. Zhao J, Simeone DM, Heidt D, Anderson MA, Lubman DM (2006) Comparative serum glycoproteomics using lectin selected sialic acid glycoproteins with mass spectrometric analysis: application to pancreatic cancer serum. J Proteome Res 5:1792–1802
187. Vanderschaeghe D, Festjens N, Delanghe J, Callewaert N (2010) Glycome profiling using modern glycomics technology: technical aspects and applications. Biol Chem 391:149–161
188. Campbell MP, Royle L, Radcliffe CM, Dwek RA, Rudd PM (2008) GlycoBase and autoGU: tools for HPLC-based glycan analysis. Bioinformatics 24:1214–1216
189. Royle L et al (2008) HPLC-based analysis of serum N-glycans on a 96-well plate platform with dedicated database software. Anal Biochem 376:1–12
190. Harvey DJ (2011) Derivatization of carbohydrates for analysis by chromatography; electrophoresis and mass spectrometry. J Chromatogr B 879:1196–1225
191. Chen X, Flynn GC (2007) Analysis of N-glycans from recombinant immunoglobulin G by on-line reversed-phase high-performance liquid chromatography/mass spectrometry. Anal Biochem 370:147–161

192. Hase S (1993) Analysis of sugar chains by pyridylamination. Methods in molecular biology (Clifton, N.J.) 14, 69–80
193. Harvey DJ (1999) Matrix-assisted laser desorption/ionization mass spectrometry of carbohydrates. Mass Spectrom Rev 18:349–450
194. Viseux N, de Hoffmann E, Domon B (1998) Structural assignment of permethylated oligosaccharide subunits using sequential tandem mass spectrometry. Anal Chem 70:4951–4959
195. Higel F, Demelbauer U, Seidl A, Friess W, Sörgel F (2013) Reversed-phase liquid-chromatographic mass spectrometric N-glycan analysis of biopharmaceuticals. Anal Bioanal Chem 405:2481–2493
196. Rocklin RD, Pohl CA (1983) Determination of carbohydrates by anion-exchange chromatography with pulsed amperometric detection. J Liq Chromatogr 6:1577–1590
197. Hagglund P, Bunkenborg J, Elortza F, Jensen ON, Roepstorff P (2004) A new strategy for identification of N-glycosylated proteins and unambiguous assignment of their glycosylation sites using HILIC enrichment and partial deglycosylation. J Proteome Res 3:556–566
198. Itoh S et al (2006) N-linked oligosaccharide analysis of rat brain Thy-1 by liquid chromatography with graphitized carbon column/ion trap-Fourier transform ion cyclotron resonance mass spectrometry in positive and negative ion modes. J Chromatogr A 1103:296–306
199. Pabst M, Bondili JS, Stadlmann J, Mach L, Altmann F (2007) Mass + retention time = structure: a strategy for the analysis of N-glycans by carbon LC-ESI-MS and its application to fibrin N-glycans. Anal Chem 79:5051–5057
200. Rohrer JS, Basumallick L, Hurum D (2013) High-performance anion-exchange chromatography with pulsed amperometric detection for carbohydrate analysis of glycoproteins. *Biochem.-Moscow* 78:697–709
201. Lee YC (1996) Carbohydrate analyses with high-performance anion-exchange chromatography. J Chromatogr A 720:137–149
202. Buszewski B, Noga S (2012) Hydrophilic interaction liquid chromatography (HILIC)—a powerful separation technique. Anal Bioanal Chem 402:231–247
203. Antonio C et al (2008) Hydrophilic interaction chromatography/electrospray mass spectrometry analysis of carbohydrate-related metabolites from Arabidopsis thaliana leaf tissue. Rapid Commun Mass Spectrom 22:1399–1407
204. Melmer M, Stangler T, Premstaller A, Lindner W (2011) Comparison of hydrophilic-interaction, reversed-phase and porous graphitic carbon chromatography for glycan analysis. J Chromatogr A 1218:118–123
205. West C, Elfakir C, Lafosse M (2010) Porous graphitic carbon: a versatile stationary phase for liquid chromatography. J Chromatogr A 1217:3201–3216
206. Karlsson NG et al (2004) Negative ion graphitised carbon nano-liquid chromatography/mass spectrometry increases sensitivity for glycoprotein oligosaccharide analysis. Rapid Commun Mass Spectrom 18:2282–2292
207. Heinisch S, Puy G, Barrioulet M-P, Rocca J-L (2006) Effect of temperature on the retention of ionizable compounds in reversed-phase liquid chromatography: application to method development. J Chromatogr A 1118:234–243
208. Ortmayr K, Hann S, Koellensperger G (2015) Complementing reversed-phase selectivity with porous graphitized carbon to increase the metabolome coverage in an on-line two-dimensional LC-MS setup for metabolomics. Analyst 140:3465–3473
209. Bajad SU et al (2006) Separation and quantitation of water soluble cellular metabolites by hydrophilic interaction chromatography-tandem mass spectrometry. J Chromatogr A 1125:76–88
210. Castagner B and Seeberger PH (2007) In: Brase S (ed) Combinatorial chemistry on solid supports, vol 278, pp 289–309. Springer-Verlag Berlin, Berlin
211. Bernardes GJL, Castagner B, Seeberger PH (2009) Combined approaches to the synthesis and study of glycoproteins. ACS Chem Biol 4:703–713
212. Hellerqvist CG (1990) In: Methods in Enzymology, vol 193, pp 554–573. Academic Press

213. Creese AJ, Cooper HJ (2012) Separation and identification of isomeric glycopeptides by high field asymmetric waveform ion mobility spectrometry. Anal Chem 84:2597–2601
214. Spina E et al (2004) New fragmentation mechanisms in matrix-assisted laser desorption/ionization time-of-flight/time-of-flight tandem mass spectrometry of carbohydrates. Rapid Commun Mass Spectrom 18:392–398
215. Konda C, Londry F, Bendiak B, Xia Y (2014) Assignment of the stereochemistry and anomeric configuration of sugars within oligosaccharides via overlapping disaccharide ladders using MSn. J Am Soc Mass Spectrom 25:1441–1450
216. Konda C, Bendiak B, Xia Y (2014) Linkage determination of linear oligosaccharides by MSn (n > 2) Collision-induced dissociation of Z(1) ions in the negative ion mode. J Am Soc Mass Spectrom 25:248–257
217. Merkle RK, Poppe I (1994) In: William GWH, Lennarz J (ed) Methods in enzymology, vol 230, pp 1–15, Academic Press
218. Xie Y, Tseng K, Lebrilla C, Hedrick J (2001) Targeted use of exoglycosidase digestion for the structural elucidation of neutral O-linked oligosaccharides. J Am Soc Mass Spectrom 12:877–884
219. Maslen S, Sadowski P, Adam A, Lilley K, Stephens E (2006) Differentiation of isomeric N-glycan structures by normal-phase liquid chromatography—MALDI-TOF/TOF tandem mass spectrometry. Anal Chem 78:8491–8498
220. Frolov A, Hoffmann P, Hoffmann R (2006) Fragmentation behavior of glycated peptides derived from D-glucose, D-fructose and D-ribose in tandem mass spectrometry. J Mass Spectrom 41:1459–1469
221. Xue J et al (2004) Determination of linkage position and anomeric configuration in Hex-Fuc disaccharides using electrospray ionization tandem mass spectrometry. Rapid Commun Mass Spectrom 18:1947–1955
222. El-Aneed A, Banoub J, Koen-Alonso M, Boullanger P, Lafont D (2007) Establishment of mass spectrometric fingerprints of novel synthetic cholesteryl neoglycolipids: the presence of a unique C-glycoside species during electrospray ionization and during collision-induced dissociation tandem mass spectrometry. J Am Soc Mass Spectrom 18:294–310
223. Xue J, Laine RA, Matta KL (2015) Enhancing MSn mass spectrometry strategy for carbohydrate analysis: A b2 ion spectral library. J. Proteomics 112:224–249
224. Ito H et al (2006) Direct structural assignment of neutral and sialylated N-glycans of glycopeptides using collision-induced dissociation MSn spectral matching. Rapid Commun Mass Spectrom 20:3557–3565
225. Konda C, Bendiak B, Xia Y (2012) Differentiation of the stereochemistry and anomeric configuration for 1-3 linked disaccharides via tandem mass spectrometry and O-18-labeling. J Am Soc Mass Spectrom 23:347–358
226. Toyama A et al (2012) Quantitative structural characterization of local N-glycan microheterogeneity in therapeutic antibodies by energy-resolved oxonium ion monitoring. Anal Chem 84:9655–9662
227. Daikoku S, Widmalm G, Kanie O (2009) Analysis of a series of isomeric oligosaccharides by energy-resolved mass spectrometry: a challenge on homobranched trisaccharides. Rapid Commun Mass Spectrom 23:3713–3719
228. Nagy G, Pohl NB (2015) Complete hexose isomer identification with mass spectrometry. J Am Soc Mass Spectrom 26:677–685
229. Hoffmann W, Hofmann J, Pagel K (2014) Energy-resolved ion mobility-mass spectrometry—a concept to improve the separation of isomeric carbohydrates. J Am Soc Mass Spectrom 1–9
230. Nagy G, Pohl NLB (2015) Monosaccharide identification as a first step toward de novo carbohydrate sequencing: mass spectrometry strategy for the identification and differentiation of diastereomeric and enantiomeric pentose isomers. Anal Chem 87:4566–4571
231. Lee S, Wyttenbach T, Bowers MT (1997) Gas phase structures of sodiated oligosaccharides by ion mobility/ion chromatography methods. Int J Mass Spectrom Ion Process 167–168:605–614

232. Fenn LS, McLean JA (2011) Structural resolution of carbohydrate positional and structural isomers based on gas-phase ion mobility-mass spectrometry. Phys Chem Chem Phys 13:2196–2205
233. Williams JP et al (2010) Characterization of simple isomeric oligosaccharides and the rapid separation of glycan mixtures by ion mobility mass spectrometry. Int J Mass Spectrom 298:119–127
234. Lundborg M, Widmalm G (2011) Structural analysis of glycans by nmr chemical shift prediction. Anal Chem 83:1514–1517
235. Barb AW, Prestegard JH (2011) NMR analysis demonstrates immunoglobulin G N-glycans are accessible and dynamic. Nat Chem Biol 7:147–153
236. Van Calsteren M-R, Gagnon F, Nishimura J, Makino S (2015) Structure determination of the neutral exopolysaccharide produced by Lactobacillus delbrueckii subsp. bulgaricus OLL1073R-1. Carbohydr Res 413:115–122
237. Wormald MR et al (2002) Conformational studies of oligosaccharides and glycopeptides: complementarity of NMR, X-ray crystallography, and molecular modelling. Chem Rev 102:371–386
238. Perez S et al (1996) Crystal and molecular structure of a histo-blood group antigen involved in cell adhesion: the Lewis x trisaccharide. Glycobiology 6:537–542
239. Rudd PM et al (1999) Roles for glycosylation of cell surface receptors involved in cellular immune recognition. J Mol Biol 293:351–366
240. Huang CY et al (2006) Carbohydrate microarray for profiling the antibodies interacting with Globo H tumor antigen. Proc. Natl. Acad. Sci. U. S. A. 103:15–20
241. Serna S, Yan S, Martin-Lomas M, Wilson IBH, Reichardt NC (2011) Fucosyltransferases as synthetic tools: glycan array based substrate selection and core fucosylation of synthetic N-glycans. J Am Chem Soc 133:16495–16502
242. Sanchez-Ruiz A, Serna S, Ruiz N, Martin-Lomas M, Reichardt NC (2011) MALDI-TOF mass spectrometric analysis of enzyme activity and lectin trapping on an array of N-glycans. Angew. Chem.-Int. Edit. 50:1801–1804
243. Bundy J, Fenselau C (1999) Lectin-based affinity capture for MALDI-MS analysis of bacteria. Anal Chem 71:1460–1463
244. Gray CJ, Weissenborn MJ, Eyers CE, Flitsch SL (2013) Enzymatic reactions on immobilised substrates. Chem. Soc, Rev
245. Love JC, Estroff LA, Kriebel JK, Nuzzo RG, Whitesides GM (2005) Self-assembled monolayers of thiolates on metals as a form of nanotechnology. Chem Rev 105:1103–1169
246. Perkins DN, Pappin DJC, Creasy DM, Cottrell JS (1999) Probability-based protein identification by searching sequence databases using mass spectrometry data. Electrophoresis 20:3551–3567
247. Hirabayashi J, Yamada M, Kuno A, Tateno H (2013) Lectin microarrays: concept, principle and applications. Chem Soc Rev 42:4443–4458